

## Stark Broadening of Neutral Helium Lines in a Plasma\*

H. R. GRIEM

*University of Maryland, College Park, Maryland, and U. S. Naval Research Laboratory, Washington, D. C.*

M. BARANGER

*Carnegie Institute of Technology, Pittsburgh, Pennsylvania*

A. C. KOLB

*U. S. Naval Research Laboratory, Washington, D. C.*

AND

G. OERTEL

*University of Maryland, College Park, Maryland*

(Received August 9, 1961)

The frequency distributions of spectral lines of nonhydrogenic atoms broadened by local fields of both electrons and ions in a plasma are calculated in the classical path approximation. The electron collisions are treated by an impact theory which takes into account deviations from adiabaticity. For the ion effects, the adiabatic approximation can be used to describe the time-dependent wave functions. The various approximations employed were examined for self-consistency, and an accuracy of about 20% in the resulting line profiles is expected. Good agreement with Wulff's experimental helium line profiles was obtained while there are large deviations from the adiabatic theory, especially for the line shifts. Asymptotic distributions for the line wings are given for astrophysical applications. Here the ion effects can be as important as the electron effects and lead to large asymmetries, but near the line core electrons usually dominate. Numerical results are tabulated for 24 neutral helium lines with principal quantum numbers up to five.

### 1. INTRODUCTION

THE Stark broadening of spectral lines by interactions of radiating atoms or ions with perturbing electrons and ions affords a sensitive method for determining plasma densities. When Stark broadening dominates the Doppler broadening, the line profiles do not depend critically on the electron and ion velocity distributions or the temperature; hence, electron densities can be inferred from line profiles without knowing the plasma temperature precisely and without invoking the assumption of local thermal equilibrium.

It is now possible to calculate the contribution of electrons to the broadening using a recently developed impact theory<sup>1,2</sup> which takes into account nonadiabatic effects due to electron collisions. The ion contribution can be treated in the usual adiabatic approximation. The theory has already been applied to the broadening of hydrogen lines,<sup>3</sup> and good agreement with the experimental profiles of Bogen<sup>4</sup> was obtained, except for the far line wings where experimental errors are quite large because of the strong continuous background. In this paper the broadening of nonhydrogenic lines arising from transitions between states where the hydrogenic degeneracy has been removed is considered. Numerical results have been obtained for 24 neutral helium lines, but the methods employed here can also be applied to a wide class of spectral lines of other

atoms. Helium was selected as an example because of its importance in stellar spectra, and because it is monatomic and convenient to use in laboratory studies for plasma density determinations. Also, it has a relatively simple electronic structure so that the wave functions can be calculated with fair accuracy.

The line broadening calculation involves three steps. First, the fluctuating microfields of the ions and electrons perturb the radiating system and this causes the wave functions (of the radiator) to be time-dependent. The perturbed wave functions are calculated here in the classical path approximation using time-dependent perturbation theory; i.e., it is shown that the perturbers can be treated as point charges moving along their classical trajectories. The validity of this assumption has been open to question so that some attention is given to justifying this approach to the problem. However, the usual assumption of adiabaticity is not required even when the classical path approximation is made.

Secondly, one must average over the various possible perturber configurations. The perturbers are assumed to be statistically independent, which can be shown to be a good approximation for nonhydrogenic isolated lines. At extremely high densities, when overlapping of different spectral lines occurs, the influence of collective effects on the microfield distribution is important as in the case of hydrogen line broadening.

Finally, the observable spectrum follows from a Fourier transform of the dipole-dipole correlation function calculated with the time-dependent perturber wave functions and averaged over the perturber trajectories.

In the case of the ion broadening the usual quasi-static approximation fails in certain cases near the

\* Jointly supported by the Office of Naval Research and the National Science Foundation.

<sup>1</sup> M. Baranger, *Phys. Rev.* **111**, 494 (1958).

<sup>2</sup> A. C. Kolb and H. Griem, *Phys. Rev.* **111**, 514 (1958).

<sup>3</sup> H. R. Griem, A. C. Kolb, and K. Y. Shen, *Phys. Rev.* **116**, 4 (1959). See also B. Mozer, Ph.D. thesis, Carnegie Institute of Technology, 1960 (unpublished); and H. R. Griem, A. C. Kolb, and K. Y. Shen, *Astrophys. J.* (January, 1962).

<sup>4</sup> P. Bogen, *Z. Physik* **149**, 62 (1957).

center of the line and the transition region between the quasi-static and impact theories must be taken into account by considering the full time-dependence of the adiabatic phase integrals. This has been done, using the Anderson-Talman<sup>5</sup> method, with the assumption that the ion perturbations are scalarly additive, which is equivalent to the binary collision assumption and, in general, leads to negligible errors since the electron broadening dominates in the line cores. This is demonstrated numerically.

For the line profiles of other light neutral atoms, validity discussions suggest that the errors in the line broadening calculations are comparable to those due to uncertainties in the atomic wave functions. The general method described here is also applicable to profiles of ion lines with certain modifications that are described in other publications.<sup>6,7</sup>

The present theory is compared with the results of earlier calculations which have been the subject of several recent review papers.<sup>8-11</sup>

## 2. GENERAL THEORY OF ELECTRON BROADENING

The electron broadening is calculated in the impact approximation. A general impact theory which allows for the possibility of overlapping lines has been developed previously.<sup>1-3</sup> Here an alternative derivation will be given which has several advantages, in particular that of clarifying the handling of weak collisions. The electrons are considered as classical particles; further discussion of this point appears later in this section. The interaction is

$$V(t) = \mathbf{e} \cdot \mathbf{E}(t), \quad (2.1)$$

where  $-\mathbf{e}r$  is the dipole moment of the atom and  $\mathbf{E}(t)$  the total electric field of all the electrons, which is the sum of the Coulomb fields of all electrons,

$$\mathbf{E}(t) = \sum_{i=1}^n \mathbf{E}_i(t), \quad (2.2)$$

$$\mathbf{E}_i(t) = \mathbf{e}r_i(t)r_i^{-3}(t). \quad (2.3)$$

The initial states are designated collectively by  $\alpha$ , and individually by  $\alpha, \alpha', \dots$ . Similarly,  $b, \beta, \beta'$  are used for the final states. Except for unimportant factors, the

line shape is given by<sup>12</sup>

$$I_{ab}(\omega) = \text{Re} \sum_{\alpha\alpha'\beta\beta'\sigma} \int_0^\infty dt \exp[i(\omega - \omega_{\alpha\beta})t] \\ \times \langle \beta | \mu_\sigma | \alpha \rangle \langle \alpha' | \mu_\sigma | \beta' \rangle \{ \langle \alpha | T_a(t, 0) | \alpha' \rangle \\ \times \langle \beta | T_b^*(t, 0) | \beta' \rangle \}_{\text{av}}, \quad (2.4)$$

where  $\mu_\sigma$  is a component of the dipole moment. The average is the thermal average over all states of the electron gas.  $T$  is the time development operator in the interaction representation, which satisfies the Schrödinger equation

$$i\hbar dT(t, t')/dt = e^{iH_0 t/\hbar} V(t) e^{-iH_0 t'/\hbar} T(t, t'). \quad (2.5)$$

$T^*$  is its complex conjugate, i.e., the transpose of its Hermitian conjugate.

Equation (2.4) is exact if quenching collisions and radiation from transitions between the sublevels,  $\alpha \rightarrow \alpha'$  and  $\beta \rightarrow \beta'$ , are neglected. To make the impact approximation, one writes

$$\Delta \{ T_a(t, 0) T_b^*(t, 0) \}_{\text{av}} \\ = \{ T_a(t + \Delta t, 0) T_b^*(t + \Delta t, 0) \\ - T_a(t, 0) T_b^*(t, 0) \}_{\text{av}} \\ = \{ [ T_a(t + \Delta t, t) T_b^*(t + \Delta t, t) - 1 ] \\ \times [ T_a(t, 0) T_b^*(t, 0) ] \}_{\text{av}}. \quad (2.6)$$

The impact approximation is valid if  $\Delta t$  can be found such that: (1)  $\Delta t$  is so large that the first factor on the right-hand side of (2.6) is statistically independent of the second factor, and the two may be averaged separately; (2)  $\Delta t$  is so small that the average of the first factor is very small compared to unity, in which case it will be shown that it can be written<sup>13</sup>

$$\exp[i(H_{0a} - H_{0b})t/\hbar] \phi_{ab} \\ \times \exp[-i(H_{0a} - H_{0b})t/\hbar] \Delta t, \quad (2.7)$$

$\phi_{ab}$  being a time-independent operator which will be calculated. Then  $\{ T_a T_b^* \}_{\text{av}}$  obeys the differential equation

$$\frac{d}{dt} \{ T_a T_b^* \}_{\text{av}} = e^{i(H_{0a} - H_{0b})t/\hbar} \phi_{ab} e^{-i(H_{0a} - H_{0b})t/\hbar} \\ \times \{ T_a T_b^* \}_{\text{av}}, \quad (2.8)$$

whose solution is

$$\{ T_a T_b^* \}_{\text{av}} = e^{i(H_{0a} - H_{0b})t/\hbar} e^{[-i(H_{0a} - H_{0b})/\hbar + \phi_{ab}]t}. \quad (2.9)$$

Substituting in Eq. (2.4) and performing the time integration, one obtains the following expression for

<sup>12</sup> Eq. (2.4) follows from Eqs. (8) and (10) of reference 1, or from Eqs. (3) and (9) of reference 3. Note that the operator called  $T$  in references 2, 3, and here, was called  $U$  in reference 1.

<sup>13</sup> The representation is always assumed to be the  $\alpha, \beta$  representation. Otherwise, various complex conjugate signs would have to be inserted. This same assumption was made in reference 3.

<sup>5</sup> P. W. Anderson, Phys. Rev. **86**, 809 (1952); and P. W. Anderson and J. D. Talman, Proceedings of the Conference on the Broadening of Spectral Lines, University of Pittsburgh, 1955 (unpublished).

<sup>6</sup> H. R. Griem and K. Y. Shen, Phys. Rev. **122**, 1490 (1961).

<sup>7</sup> M. Baranger and J. C. Stewart (to be published).

<sup>8</sup> R. G. Breene, Revs. Modern Phys. **29**, 94 (1957).

<sup>9</sup> S. Chen and M. Takeo, Revs. Modern Phys. **29**, 20 (1957).

<sup>10</sup> H. Margenau and M. Lewis, Revs. Modern Phys. **31**, 569 (1959).

<sup>11</sup> G. Traving, *Über die Theorie der Druckverbreiterung von Spektrallinien* (Verlag G. Braun, Karlsruhe, 1960).

the line shape<sup>14</sup>:

$$I_{ab}(\omega) = -\text{Re} \sum_{\alpha\alpha'\beta\beta'\sigma} \langle \beta | \mu_\sigma | \alpha \rangle \langle \alpha' | \mu_\sigma | \beta' \rangle \\ \times \langle \alpha | \langle \beta | [i\omega - i(H_{0a} - H_{0b})/\hbar + \phi_{ab}]^{-1} | \alpha' \rangle | \beta' \rangle. \quad (2.10)$$

The contention is that the impact approximation is valid when

$$erE\tau \ll 1, \quad (2.11)$$

where  $er$  is a typical matrix element of the dipole moment,  $E$  a typical electric field (say, the Holtmark normal field strength  $2.61 eN^{2/3}$ ), and  $\tau$  a typical correlation time for the time-dependence of the electric field. The latter is at most equal to the Debye length divided by the velocity, i.e., the reciprocal of the plasma frequency  $\omega_p = (4\pi N e^2/m)^{1/2}$ . The first condition on  $\Delta t$  can be satisfied by picking it appreciably larger than  $\tau$ . Equation (2.11) makes it possible to satisfy also the second condition, since every term, except the first, in the perturbation expansion of  $T(t+\Delta t, t)$ , with  $\hbar\omega_{\alpha\alpha'} \equiv \langle \alpha | H_{0a} | \alpha \rangle - \langle \alpha' | H_{0a} | \alpha' \rangle$ , etc.,

$$\langle \alpha | T_a(t+\Delta t, t) | \alpha' \rangle \\ = \langle \alpha | \alpha' \rangle - \frac{i}{\hbar} \int_t^{t+\Delta t} du \exp(i\omega_{\alpha\alpha'}u) \langle \alpha | V(u) | \alpha' \rangle \\ - \frac{1}{\hbar^2} \sum_{\alpha''} \int_t^{t+\Delta t} du_1 \int_t^{u_1} du_2 \\ \times \exp(i\omega_{\alpha\alpha''}u_1 + i\omega_{\alpha''\alpha'}u_2) \langle \alpha | V(u_1) | \alpha'' \rangle \\ \times \langle \alpha'' | V(u_2) | \alpha' \rangle + \dots, \quad (2.12)$$

can be made small compared to unity most of the time by proper choice of  $\Delta t$ , justifying the replacement of the difference Eq. (2.6) by the differential Eq. (2.8). With this expansion, the average of the first factor on the right side of Eq. (2.6) is

$$\langle \alpha | \langle \beta | \{ T_a(t+\Delta t, t) T_b^*(t+\Delta t, t) - 1 \}_{av} | \alpha' \rangle | \beta' \rangle \\ = \sum_{m=1}^{\infty} \sum_{k=1}^{\infty} \left( -\frac{i}{\hbar} \right)^m \left( \frac{i}{\hbar} \right)^k \sum_{\alpha'' \dots \beta'' \dots} \int_t^{t+\Delta t} du_1 \dots \\ \times \int_t^{u_{m-1}} du_m \int_t^{t+\Delta t} d\mathbf{w}_1 \dots \int_t^{w_{k-1}} d\mathbf{w}_k \\ \times \exp[i\omega_{\alpha\alpha''}u_1 + \dots + i\omega_{\alpha''\alpha'}u_m \\ - i\omega_{\beta\beta''}w_1 - \dots - i\omega_{\beta''\beta'}w_k] \\ \times \{ \langle \alpha | V(u_1) | \alpha'' \rangle \dots \langle \dots | V(u_m) | \alpha' \rangle \\ \times \langle \beta | V(\mathbf{w}_1) | \beta'' \rangle^* \dots \langle \dots | V(\mathbf{w}_k) | \beta' \rangle^* \}_{av}. \quad (2.13)$$

The summation involves only even values of  $m+k$ ; odd terms average to zero because the perturbation (2.1) is an odd function of the perturber coordinates. For long-range forces, because of condition (2.11),

<sup>14</sup> This is Eq. (62) of reference 1 and Eq. (10) of reference 3.

terms with  $m+k=2$  will be the only important ones most of the time and others can be neglected. Once in a while, however, an electron comes very close to the atom and creates a huge electric field. Then, higher-order terms are important. But, when this happens, correlations are not important and the fields of all the other electrons can be neglected compared to that of the close one. Hence, in the terms with  $m+k \geq 4$ , the total electric field can be replaced by the field of a single electron, say electron 1, and the result then be multiplied by  $n$ , the total number of electrons. This cannot be done for the lowest-order term, because weak fields are influenced to some extent by the correlations between electrons. One can, however, replace one of the two fields in the second-order term by the field of electron 1 and multiply by  $n$ ; this amounts to saying that all electrons are equivalent, a triviality. But the second field must remain the total field.

The thermal average is performed in two steps. First, the position and velocity of electron 1 at a certain time are fixed and the average is over the motions of the other electrons. Second, one averages over the paths of electron 1 itself. The first step does not affect the higher-order terms at all, since they contain only the field of electron 1. It does affect the second-order terms, however. The problem is: knowing that electron 1 is at  $\mathbf{r}$ , with velocity  $\mathbf{v}$ , at time  $t$ , what is the average total electric field at the origin at time  $t'$ ? The answer is some sort of shielded field which exists only in the vicinity of electron 1. As a first approximation, one may assume that the electron moves along a straight trajectory at constant speed and uses the Debye shielded field. This is correct for particles which do not have too high a velocity. For the high-velocity particles, the Debye sphere is distorted. The effect of long-range correlations on the electric field autocorrelation function can be computed by a method of Rostoker<sup>15</sup> that takes into account the distortion of the Debye sphere. However, because the  $\phi$ -matrix elements depend inversely on the particle velocities for situations where shielding is important, the low-velocity part of the electron velocity distribution gives the dominant contribution to the broadening and the Debye approximation is valid. In conclusion, one can use fields of a single electron in the second-order term too, one of them being a Debye shielded field and the other unshielded.

To perform the second step of the average, electron 1 is again taken to follow a straight path at constant speed. The variables are: the impact parameter  $\rho$ ; the speed  $v$ ; the time of closest approach  $s$ ; various angles. The average is given by

$$V^{-1} \int_0^{\infty} f(v) dv \int_0^{\infty} 2\pi\rho d\rho \int_{-\infty}^{+\infty} v ds \\ \times \{ T_a(t+\Delta t, t) T_b^*(t+\Delta t, t) - 1 \}, \quad (2.14)$$

<sup>15</sup> N. Rostoker, Bull. Am. Phys. Soc. 5, 364 (1960).

where  $\{ \}$  indicates from now on the average over angles;  $f(v)$  is the Maxwell distribution and  $V$  the volume of the box, which combines with the factor  $n$  to give  $N$ , the electron density. The integrand in (2.13) is appreciable<sup>16</sup> only if all times occur within interval  $\tau$  of each other and of the time of closest approach,<sup>17</sup> where  $\tau$  is again the maximum correlation time. Since  $\Delta t$  is much larger than  $\tau$ , two kinds of collisions can be distinguished: those for which the time of closest approach  $s$  falls outside of the interval  $(t, t+\Delta t)$ , whose contribution can be neglected; and those for which  $t < s < t+\Delta t$ . For the latter, one can set  $t = -\infty$  and  $t+\Delta t = +\infty$  without appreciably changing the integral.<sup>17</sup> This is analogous to the phase shift limit of the usual adiabatic theory. Thus, (2.13) can be expressed in terms of the  $S$  matrix<sup>18</sup> for a single collision taking place at time  $s$ ,  $S = T(+\infty, -\infty)$ ,

$$\begin{aligned} \langle \alpha | S_a | \alpha' \rangle &= \langle \alpha | \alpha' \rangle \\ &- \frac{ie}{\hbar} \sum_{\sigma} \langle \alpha | r_{\sigma} | \alpha' \rangle \int_{-\infty}^{\infty} e^{i\omega_{\alpha\alpha'} u} E_{1\sigma}(u) du \\ &- \frac{e^2}{\hbar^2} \sum_{\sigma\nu\alpha''} \langle \alpha | r_{\sigma} | \alpha'' \rangle \langle \alpha'' | r_{\nu} | \alpha' \rangle \\ &\times \int_{-\infty}^{\infty} du_1 \int_{-\infty}^{u_1} du_2 e^{i(\omega_{\alpha\alpha''} u_1 + \omega_{\alpha''\alpha'} u_2)} \\ &\times E_{1\sigma}(u_1) E_{1\nu}(u_2) + \dots \quad (2.15) \end{aligned}$$

This is easily seen to be related to the  $S$  matrix for a collision taking place at time  $t=0$  by

$$\langle \alpha | S_a(s) | \alpha' \rangle = e^{i\omega_{\alpha\alpha'} s} \langle \alpha | S_a(0) | \alpha' \rangle. \quad (2.16)$$

But (2.16) is really independent of  $s$  as long as  $< s < t+\Delta t$ , because  $\omega_{\alpha\alpha'} \Delta t$  is very small. This follows from the facts that two states  $\alpha$  and  $\alpha'$  will give rise to overlapping lines only if  $\omega_{\alpha\alpha'}$  is of the order of the width of the lines, and that the product of the width by  $\Delta t$  is small as a result of the second condition imposed earlier on  $\Delta t$ . Hence  $s$  on the right-hand side of (2.16) can be replaced by  $t$ . Then the integral over  $s$  in (2.14) can be replaced by  $\Delta t$  and one obtains (2.7) with<sup>19</sup>

$$\phi_{ab} = N \int_0^{\infty} v f(v) dv \int_0^{\infty} 2\pi\rho d\rho \{ S_a(0) S_b^*(0) - 1 \}. \quad (2.17)$$

The average over angles eliminates all terms containing an odd number of electric fields. And it must be remembered that, in the second-order terms, one of the fields should be shielded and the other unshielded. If two unshielded fields are used, the integral over  $\rho$  may

diverge for large  $\rho$ . It is convenient to use two unshielded fields and to introduce an equivalent cutoff in the  $\rho$  integration. It is shown in Appendix X that the cutoff should be made at 1.1 times the Debye length, if one uses the Debye shielded field.

Thus, the problem of electron broadening is reduced to the calculation of the  $S$  matrix for a single scattering. Here, the electrons have been treated classically, but Eqs. (2.10) and (2.17) are also valid when their motion is treated quantum mechanically,<sup>20</sup> provided that the integral over impact parameters be replaced by a sum over  $l$  values, and the classical path  $S$  matrix by the appropriate matrix element of the fully quantum mechanical one. The classical treatment is valid whenever a large number of  $l$  values contribute to the answer.<sup>21</sup> This allows one to replace the sum over  $l$  by an integration; it also means that the potentials vary so smoothly that the matrix elements of the quantum mechanical  $S$  matrix can be calculated in the WKB approximation, which is equivalent to using classical trajectories. If in addition, straight trajectories are to be used, the interaction energy must be small compared to the energy of the electrons. Both these conditions are realized in the applications to neutral helium lines that will be given here. In the case of lines emitted by ions, it may be necessary to use hyperbolic classical trajectories to take into account the Coulomb interaction. This has been done for a number of cases where it was found that the effect can either increase or decrease the broadening.<sup>6,7</sup> For ionized helium lines,<sup>6</sup> the corrections are small for temperatures from 5000–80 000 °K and densities from  $10^{15}$ – $10^{19}$  cm<sup>-3</sup>.

### 3. ELECTRON BROADENING OF ISOLATED LINES

Equation (2.10) is the general result to be used in all cases where electron broadening is treated by the impact approximation. It applies to overlapping as well as isolated lines. In many of the applications to helium lines the line is isolated and the only degeneracy is that associated with the magnetic quantum numbers; moreover, the final state is usually much less polarizable than the initial state, so that its interaction with the electrons can be neglected. Then  $S_b^*(0)$  can be replaced by unity in Eq. (2.17), and the resulting  $\phi_a$  is just a

<sup>20</sup> M. Baranger, Phys. Rev. **112**, 855 (1958).

<sup>21</sup> In the recent article by H. Margenau and M. Lewis, reference 10, some doubts were expressed about the validity of the classical path treatment even under these conditions. The conclusion, as expressed in Eq. (2.11) of this reference, is essentially that the classical treatment is not valid whenever the impact approximation holds. That this must be erroneous is clear since, in simple cases [E. Lindholm, dissertation, Uppsala (1942); M. Baranger, Phys. Rev. **111**, 481 (1958); H. R. Griem and K. Y. Shen, Phys. Rev. **122**, 1490 (1961)], the identity of the classical impact and quantum mechanical impact treatments is easily established. The fallacy resides in Eq. (2.6) of reference 10 which is needlessly restrictive and where  $d$  should be replaced by  $r$ . The condition (2.9a) in this reference is also unnecessary, since the problem at hand is not that of calculating the precise angle by which the electron is scattered, but only the effect that the presence of the electron has upon light.

<sup>16</sup> The following argument is due to B. Mozer (reference 3).

<sup>17</sup> This is true even of the second-order terms because of shielding.

<sup>18</sup> This operator was called  $T$ ; in references 2 and 3.

<sup>19</sup> This is Eq. (61) of reference 1 and Eq. (7) of reference 3.

multiple of the unit matrix because of spherical symmetry. The sums over  $\sigma, \beta', \beta''$  in Eq. (2.10) also give a multiple of the unit matrix in  $\alpha, \alpha'$ . Hence, the line shape is Lorentzian as in Anderson's impact theory.<sup>22</sup> When normalized to  $\int I(\omega)d\omega=1$  it is

$$I_\alpha(\omega) = - (1/\pi) \operatorname{Re}[i\omega - i\omega_{\alpha\beta} + \langle \alpha | \phi_\alpha | \alpha \rangle]^{-1} \\ = (w/\pi) [(\omega - \omega_{\alpha\beta} - d)^2 + w^2]^{-1}, \quad (3.1)$$

with

$$w = -\operatorname{Re}\langle \alpha | \phi_\alpha | \alpha \rangle, \quad (3.2) \\ d = -\operatorname{Im}\langle \alpha | \phi_\alpha | \alpha \rangle,$$

and from Eq. (2.17)

$$\langle \alpha | \phi_\alpha | \alpha \rangle = N \int v f(v) dv \int 2\pi \rho d\rho \{ \langle \alpha | S_\alpha(0) - 1 | \alpha \rangle \}. \quad (3.3)$$

According to Eq. (2.15) without the fourth and higher-order terms, one has

$$\{ \langle \alpha | S_\alpha(0) - 1 | \alpha \rangle \} = - \left\{ \frac{e^2}{\hbar^2} \sum_{\sigma\nu\alpha'} \langle \alpha | r_\sigma | \alpha' \rangle \langle \alpha' | r_\nu | \alpha \rangle \right. \\ \left. \times \int_{-\infty}^{\infty} du_1 \int_{-\infty}^{u_1} du_2 \exp[i(\omega_{\alpha\alpha'} u_1 + \omega_{\alpha'\alpha} u_2)] \right. \\ \left. \times E_{1\sigma}(u_1) E_{1\nu}(u_2) + \dots \right\}. \quad (3.4)$$

With Eq. (2.3) and  $r_{1\sigma}(u) = \rho_{1\sigma} + v_{1\sigma}u$ , this can be written

$$\{ \langle \alpha | S_\alpha(0) - 1 | \alpha \rangle \} = - \frac{e^4}{\hbar^2} \left\{ \sum_{\sigma\nu\alpha'} \langle \alpha | r_\sigma | \alpha' \rangle \langle \alpha' | r_\nu | \alpha \rangle \right. \\ \left. \times \int_{-\infty}^{+\infty} du_1 \int_{-\infty}^{u_1} du_2 \exp[i(\omega_{\alpha\alpha'} u_1 + \omega_{\alpha'\alpha} u_2)] \right. \\ \left. \times \frac{\rho_{1\sigma}\rho_{1\nu} + v_{1\sigma}v_{1\nu}u_1u_2}{|r_1(u_1)|^3 |r_1(u_2)|^3} \right\} + \dots, \quad (3.5)$$

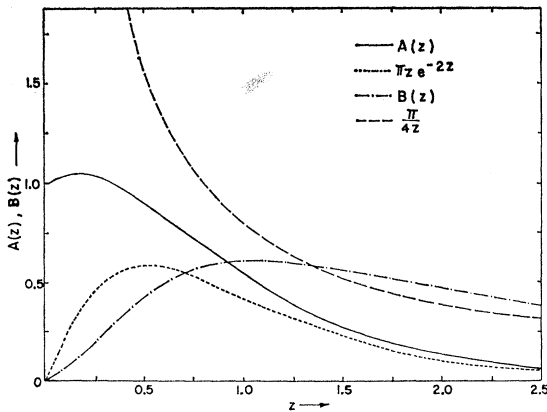


FIG. 1. The functions  $A(z)$  and  $B(z)$  and their asymptotic representations.

<sup>22</sup> P. W. Anderson, Phys. Rev. **76**, 647 (1949).

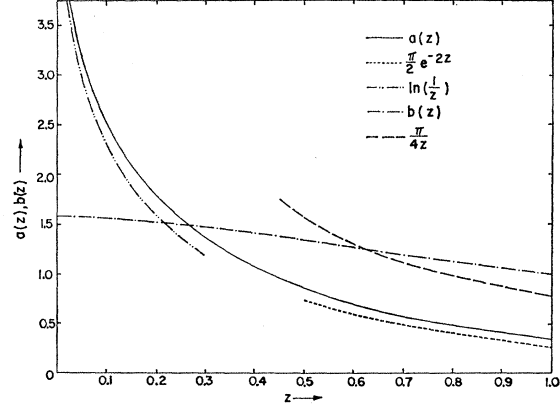


FIG. 2. The functions  $a(z)$  and  $b(z)$  and their asymptotic representations.

because terms containing  $\rho_{1\sigma}v_{1\nu}$  will average out. For  $\sigma \neq \nu$ ,  $\rho_{1\sigma}\rho_{1\nu}$  and  $v_{1\sigma}v_{1\nu}$  also give zero in the average. Using  $\{\rho_{1\sigma}\rho_{1\sigma}\} = \frac{1}{3}\rho^2$ ,  $\{v_{1\sigma}v_{1\sigma}\} = \frac{1}{3}v^2$ , and  $|r_1|^2 = \rho^2 + v^2u^2$ , one has with the definitions  $z_{\alpha\alpha'} \equiv \omega_{\alpha\alpha'}/v$  and  $x \equiv vu/\rho$ ,

$$\{ \langle \alpha | S_\alpha - 1 | \alpha \rangle \} = - \frac{1}{3} \left( \frac{e^2}{\hbar\rho v} \right)^2 \sum_{\sigma\alpha'} \langle \alpha | r_\sigma | \alpha' \rangle \langle \alpha' | r_\sigma | \alpha \rangle \\ \times \int_{-\infty}^{+\infty} dx_1 \int_{-\infty}^{x_1} dx_2 \exp[iz_{\alpha\alpha'}(x_1 - x_2)] \\ \times \frac{1 + x_1x_2}{(1 + x_1^2)^{3/2} (1 + x_2^2)^{3/2}} + \dots \\ \equiv - \frac{2}{3} \left( \frac{e^2}{\hbar\rho v} \right)^2 \sum_{\sigma\alpha'} \langle \alpha | r_\sigma | \alpha' \rangle \langle \alpha' | r_\sigma | \alpha \rangle \\ \times [A(z_{\alpha\alpha'}) + iB(z_{\alpha\alpha'})] + \dots. \quad (3.6)$$

As shown in Appendix Y, the integrations over  $x_1$  and  $x_2$  can be expressed in terms of Bessel functions:

$$A(z) = z^2 [K_0^2(|z|) + K_1^2(|z|)], \quad (3.7)$$

and the principal value integral ( $P$ )

$$B(z) = -P \int_0^\infty \frac{A(z')}{z^2 - z'^2} dz', \quad (3.8)$$

where  $K_0(z)$  and  $K_1(z)$  vanish exponentially for large  $z$  values.<sup>23</sup>  $A(z)$  and  $B(z)$ , which are needed for the following numerical integrations, and their asymptotic approximations are exhibited in Fig. 1. Note also that  $A(z)$  is an even function and  $B(z)$  an odd function of  $z$ . The integration over  $\rho$  involves the functions

$$a(z) \equiv \int_z^\infty \frac{A(z')}{z'} dz', \quad b(z) \equiv \int_z^\infty \frac{B(z')}{z'} dz', \quad (3.9)$$

<sup>23</sup> Basset, Proc. Cambridge Phil. Soc. **6**, 11 (1889); see also G. N. Watson, *Theory of Bessel Functions* (Cambridge University Press, New York, 1952), 2nd ed., p. 78.

which are shown in Fig. 2. (See Appendix Y for mathematical details.)

With these definitions the contribution of weak collisions, for which terms of higher than second order are negligible, to the  $\phi$ -matrix element can be written

$$\langle \alpha | \phi_a | \alpha \rangle_w = -(4\pi/3)(e^2/\hbar)^2 N \times \int \frac{dv}{v} f(v) \sum_{\sigma\sigma'} |\langle \alpha | r_\sigma | \alpha' \rangle|^2 \times [a(z_{\alpha\alpha'}^{\min}) + ib(z_{\alpha\alpha'}^{\min})], \quad (3.10)$$

where  $z_{\alpha\alpha'}^{\min} \equiv \omega_{\alpha\alpha'} \rho_{\min}/v$  corresponds to a minimum impact parameter, at which the perturbation theory breaks down. The effect of strong collisions can be estimated by the Lorentz term (assuming complete interruption of the radiation)

$$\langle \alpha | \phi_a | \alpha \rangle_s \approx -N \int dv f(v) v \pi \rho_{\min}^2(v). \quad (3.11)$$

In the high-temperature limit ( $z_{\alpha\alpha'}^{\min} \rightarrow 0$ ), Eqs. (Y15) and (Y16) may be used and one obtains with  $a_0 = \hbar^2/mv^2$

$$\langle \alpha | \phi_a | \alpha \rangle_\infty = \langle \alpha | \phi_a | \alpha \rangle_s - \frac{4\pi}{3} \left(\frac{\hbar}{m}\right)^2 N \int \frac{dv}{v} f(v) \sum_{\sigma\sigma'} \left| \frac{\langle \alpha | r_\sigma | \alpha' \rangle}{a_0} \right|^2 \times [\ln(|z_{\alpha\alpha'}^{\min}|^{-1}) \pm i\pi/2], \quad (3.12)$$

where the signs of the contributions to the shift are determined by those of the  $\omega_{\alpha\alpha'}$ . In this case

$$[A(z_{\alpha\alpha'}^{\min}) \approx 1, B(z_{\alpha\alpha'}^{\min}) \approx 0],$$

the condition for the validity of the perturbation theory is particularly simple, namely

$$|\{\langle \alpha | S_a(\rho_{\min}) - 1 | \alpha \rangle\}| \approx \frac{2}{3} \left(\frac{\hbar}{mv\rho_{\min}}\right)^2 \sum_{\sigma\sigma'} \left| \frac{\langle \alpha | r_\sigma | \alpha' \rangle}{a_0} \right|^2 \approx \frac{2}{3} \left(\frac{\hbar}{mv\rho_{\min}}\right)^2 a^4 \approx 1. \quad (3.13)$$

(Here,  $a$  is the principal quantum number of the upper state.) The minimum impact parameter is accordingly inversely proportional to the velocity, and the strong collision term in Eq. (3.12) is entirely negligible, i.e., perturbation theory gives the exact answer in the high-temperature limit.

Also for the opposite extreme (low-temperature limit) an exact result is available from the adiabatic impact theory, which can be worked out to all orders

(see the following section):

$$\langle \alpha | \phi | \alpha \rangle_0 = \left(\frac{\pi}{2}\right)^{5/3} \frac{\Gamma(\frac{1}{3})}{3^{2/3}} \left(\frac{\hbar}{m}\right)^{4/3} N \times \left(\sum_{\sigma\sigma'} \frac{1}{\omega_{\alpha\alpha'}} \left| \frac{\langle \alpha | r_\sigma | \alpha' \rangle}{a_0} \right|^2\right)^{3/2} \langle v^3 \rangle_{av} (1 \pm i\sqrt{3}). \quad (3.14)$$

In the intermediate range (the usual situation), appropriate estimates for the strong collision term and the limiting impact parameter must be used. One possible set of equations which properly reduce to both limits is

$$\langle \alpha | \phi_a | \alpha \rangle_1 = -N \int dv f(v) \left\{ \pi v \rho_{\min}^2 + \frac{4\pi}{3v} \left(\frac{\hbar}{m}\right)^2 \times \sum_{\sigma\sigma'} \left| \frac{\langle \alpha | r_\sigma | \alpha' \rangle}{a_0} \right|^2 [a(z_{\alpha\alpha'}^{\min}) + ib(\frac{3}{4}z_{\alpha\alpha'}^{\min})] \right\}, \quad (3.15)$$

where  $\rho_{\min} = z_{\alpha\alpha'}^{\min} v / \omega_{\alpha\alpha'}$  is defined by

$$|\{\langle \alpha | S_a(\rho_{\min}) - 1 | \alpha \rangle\}| \approx \frac{2}{3} \left(\frac{\hbar}{mv\rho_{\min}}\right)^2 \left[ \left(\sum_{\sigma\sigma'} \left| \frac{\langle \alpha | r_\sigma | \alpha' \rangle}{a_0} \right|^2 A(z_{\alpha\alpha'}^{\min})\right)^2 + \left(\sum_{\sigma\sigma'} \left| \frac{\langle \alpha | r_\sigma | \alpha' \rangle}{a_0} \right|^2 B(z_{\alpha\alpha'}^{\min})\right)^2 \right]^{-1/2} = \left[\frac{1}{2}\Gamma(\frac{1}{3})\right]^{-3} \approx \left(\frac{3}{4}\right)^{3/2}. \quad (3.16)$$

Here for the widths, the strong and weak collision terms of Eqs. (3.10) and (3.11) are preserved, and agreement with the limiting cases is achieved by choosing different cutoffs in width and shift and by the choice of the numerical value of Eq. (3.16), which defines the impact parameter at which the perturbation theory fails.

An alternative cutoff procedure is to use

$$\langle \alpha | \phi_a | \alpha \rangle_2 = -N \int dv f(v) \left\{ \left(\frac{4}{3}\right)^{3/2} \pi v \rho_{\min}^2 + \frac{4\pi}{3v} \left(\frac{\hbar}{m}\right)^2 \sum_{\sigma\sigma'} \left| \frac{\langle \alpha | r_\sigma | \alpha' \rangle}{a_0} \right|^2 [a(z_{\alpha\alpha'}^{\min}) + (\frac{4}{3})^{3/2} ib(z_{\alpha\alpha'}^{\min})] \right\}, \quad (3.17)$$

and an equation like (3.16) with  $(3/4)^{3/2}$  replaced by  $\sqrt{3}/2$ , which, however, only reduce to the adiabatic limit (using again  $\frac{1}{2}\Gamma(\frac{1}{3}) = 1.339 \dots \approx \frac{4}{3}$ ). Here a single cutoff in the real and imaginary parts is employed, but an ad hoc correction factor  $(4/3)^{3/2} \approx 1.21$  had to be inserted in the strong collision term and the shift.

The deviation of the correction factor in Eq. (3.17) from unity may be considered as an indication of the

uncertainties introduced by the schematic treatment of the strong collisions, i.e., the second set of equations exhibits more clearly the limitations inherent in this treatment. The largest differences between the two proposed procedures are expected at high velocities, because they both reduce to the adiabatic theory result for small velocities. But for large velocities the width is dominated by the weak collision term, which depends only logarithmically on the cutoff, and therefore Eqs. (3.15) and (3.17) give practically the same widths. Only the shift is seriously affected; it is a factor 1.21 too large in the second case. However, in this limit, the shift is smaller than the width, and if the shift is expressed dimensionlessly in terms of the width the two procedures should only deviate by  $<20\%$ . This was borne out by comparing numerical results for the 24 helium lines. Further insight into the errors introduced by the use of cutoffs may be gained by subjecting calculated widths and shifts to a quantum mechanical dispersion relation.<sup>24</sup>

It may be surprising that sufficient accuracy is obtained from a perturbation treatment in which only the first nonvanishing term is considered. The explanation is that because of the long-range nature of the interaction for high electron velocities, most of the broadening is due to the distant collisions whose contribution is accurately described by the second-order term in the perturbation solution of the Schrödinger equation. Strong collisions usually only account for approximately 20% of the electron broadening, and the uncertainty in the strong collision term (probably good to within a factor 2) should therefore produce errors of about 10% in terms of the total width. For smaller electron velocities strong collisions are more important. However, this does not lead to large errors because the cutoff procedure was chosen in such a way as to yield the adiabatic result, which is correct to all orders. This is quite different from cases where the line broadening is due to interactions with neutral perturbers. Then the short-range forces cause the strong collisions to dominate, and no satisfactory results can be obtained from just the leading term in the perturbation expansion.

At high electron densities and in case of closely spaced levels, the above equations will tend to overestimate the broadening and shift because screening was neglected. But under such conditions, one can use the  $\phi$ -matrix elements for hydrogen,<sup>3</sup> which were derived taking into account the Debye screening. These  $\phi$ -matrix elements [Eq. (29) of reference 3] should accordingly be used instead of those given by Eqs. (3.12), (3.15), or (3.17) in cases for which the latter yield larger results, that is, for densities larger than  $N_{\max}$  defined by

$$a(z_{\alpha\alpha'}^{\min}) \approx \ln(v/\omega_{\alpha\alpha'}\rho_{\min}) \approx \ln(\rho_D/\rho_{\min}), \quad (3.18)$$

<sup>24</sup>H. R. Griem and C. S. Shen, following paper [Phys. Rev. 125, 196 (1962)].

since the  $\phi$  matrix depends logarithmically on the cutoff in both instances. With  $\rho_D = (kT/4\pi e^2 N)^{1/2}$  and  $(1/v)_{av} = (2m/\pi kT)^{1/2}$  (the  $\phi$ -matrix elements are inversely proportional to the velocity) this yields the critical density

$$N_{\max} \approx m\omega_{\alpha\alpha'}^2/2\pi^2 e^2. \quad (3.19)$$

For typical values of the splitting  $\omega_{\alpha\alpha'} \approx 10^{14} \text{ sec}^{-1}$ , the  $\phi$ -matrix elements which were derived taking into account the splitting but neglecting the Debye-screening are therefore applicable for electron densities below  $N_{\max} \approx 2 \times 10^{18} \text{ cm}^{-3}$ , i.e., almost in the whole range in which isolated lines can be observed. That these formulas only yield diagonal elements is no serious restriction because off-diagonal elements are of interest only in case of overlapping lines, i.e., small splittings and high densities, where the hydrogen formula is valid. It is interesting to note that Eq. (3.19) is equivalent to saying that at the critical density the plasma frequency is comparable to the splitting.

#### 4. ION AND ELECTRON BROADENING OF ISOLATED LINES

The ion velocities are usually small enough that the adiabatic approximation is valid. In the general formula for the profile of a spectral line due to dipole radiation (2.4), the average over the perturbers of the  $T_a T_b^*$  operators splits into two factors, if electron and ion perturbations are independent. The ion factor is given in terms of the usual phase integral

$$\{T_a(t,0)T_b^*(t,0)\}_{\text{ions}} = \left\{ \exp \left[ -i \int_0^t \Delta\omega_{ab}(t') dt' \right] \right\}, \quad (4.1)$$

where  $\Delta\omega_{ab}$  is the instantaneous shift due to the ion field. According to the previous section, the electron contribution is

$$\begin{aligned} \{T_a(t,0)T_b^*(t,0)\}_{\text{electrons}} &= \exp(\phi_{ab}t) \\ &= \exp[-(w+id)t]. \end{aligned} \quad (4.2)$$

( $\phi_{ab}$  is never affected by the ion field because this causes in case of quadratic Stark effect only shifts much smaller than the splitting of the interacting levels, and because in case of linear Stark effect  $\phi_{ab}$  is independent of the splitting<sup>3</sup>)

The phase integral in Eq. (4.1) can be calculated provided that two approximations are made; namely, (1) the individual ion perturbations do not overlap in time so that they are scalarly additive, i.e.,  $\Delta\omega_{ab}$  is a sum of contributions from single ions,

$$\Delta\omega_{ab}(t) = \sum_j [\Delta\omega_{ab}(t)]_j,$$

and (2) the adiabatic approximation is also valid near the line center where the usual statistical theory fails. The first approximation does not cause serious errors because in the line center, where the impact approximation is valid, the binary collision assumption also applies as the interactions are weak; while on the line

wing the assumption of scalar additivity does not change the asymptotic behavior of the true field distribution, because this behavior is due to a single ion coming very close. In the intermediate regime, the assumption of scalar additivity breaks down, but here the profile is dominated by electron broadening.

The adiabatic assumption is always valid for the ion broadening of isolated lines. Therefore, omitting the dipole matrix elements, one can write

$$I(\omega) = \frac{1}{\pi} \operatorname{Re} \left\{ \int_0^\infty dt \exp[i(\omega-d)t - wt] -i \sum_j P_j(t) \right\}, \quad (4.3)$$

where  $P_j(t)$  is the phase integral for the  $j$ th ion. With the time-independent perturbation theory result (averaged over the magnetic quantum numbers, i.e., neglecting the small splitting of the levels with different  $m$  by the ion field),

$$\Delta\omega_{ab} = \frac{2\pi C_4}{r^4} = \frac{1}{3r^4} \left( \frac{\hbar}{m} \right)^2 \sum_{\sigma\alpha'} \frac{1}{\omega_{\alpha\alpha'}} \left| \frac{\langle \alpha | r_\sigma | \alpha' \rangle}{a_0} \right|^2,$$

this is, using  $r_j^2 = \rho_j^2 + v^2(t-t_j)^2$ , given by

$$P_j(t) = \int_0^t \Delta\omega_{ab}(t') dt' \\ = \frac{\pi C_4}{\rho_j^3 v} \left[ \tan^{-1} \left( \frac{v(t-t_j)}{\rho_j} \right) + \tan^{-1} \left( \frac{vt_j}{\rho_j} \right) + \frac{\rho_j v(t-t_j)}{\rho_j^2 + v^2(t-t_j)^2} + \frac{\rho_j vt_j}{\rho_j^2 + v^2 t_j^2} \right]. \quad (4.4)$$

Because of the assumptions of scalar additivity and statistical independence the ion contribution becomes in the usual way<sup>5</sup>

$$\{\exp[-i \sum_j P_j(t)]\} = \{\exp[-iP_1(t)]\}^n \\ = (1 + \{\exp[-iP_1(t)] - 1\})^n \xrightarrow{n \rightarrow \infty} \\ \exp(NV\{\exp[-iP_1(t)] - 1\}), \quad (4.5)$$

$n$  being the total number of ions,  $N$  the ion density, and  $V$  the volume. The average can be expressed by

$$2\pi v \int dt_1 \int \rho_1 d\rho_1 (\exp[-iP_1(t)] - 1) \left( 2\pi v \int dt_1 \int \rho_1 d\rho_1 \right)^{-1} \\ = 2\pi v V^{-1} \int dt_1 \int d\rho_1 \rho_1 (\exp[-iP_1(t)] - 1), \quad (4.6)$$

so that finally

$$\{\exp[-i \sum_j P_j(t)]\} = \exp \left[ 2\pi N v \int_{-\infty}^\infty dt_1 \right. \\ \left. \times \int_0^\infty d\rho_1 \rho_1 (\exp[-iP_1(t)] - 1) \right]. \quad (4.7)$$

One then introduces

$$r = \rho_1 / \rho_m, \quad \delta = w t_1, \quad \tau = w t, \quad \sigma = w \rho_m / v, \\ (4\pi/3) \rho_m^3 N = 1, \quad (4.8) \\ x = (\omega - d) / w, \quad \alpha = (2\pi C_4 / w \rho_m^4)^{\frac{1}{2}};$$

and in terms of these quantities the profile is given by

$$j(x, \alpha, \sigma) = \frac{1}{\pi} \int_0^\infty d\tau \exp[ix\tau - \tau + g(\tau, \alpha, \sigma)], \quad (4.9)$$

where

$$g(\tau, \alpha, \sigma) = \frac{3}{2\sigma} \int_0^\infty r dr \int_{-\infty}^\infty d\delta \left\{ \exp \left[ -i\alpha^{\frac{1}{2}} \frac{\sigma}{2r^3} \right. \right. \\ \left. \left. \times \left( \tan^{-1} \left( \frac{\tau - \delta}{r\sigma} \right) + \tan^{-1} \left( \frac{\delta}{r\sigma} \right) + \frac{(\tau - \delta)r\sigma}{(r\sigma)^2 + (\tau - \delta)^2} \right. \right. \right. \\ \left. \left. \left. + \frac{\delta r\sigma}{(r\sigma)^2 + \delta^2} \right) \right] - 1 \right\}. \quad (4.10)$$

For small ion velocities the function  $j(x, \alpha, \sigma)$  reduces to<sup>25</sup>

$$\lim_{\sigma \rightarrow \infty} j(x, \alpha, \sigma) = \frac{1}{\pi} \operatorname{Re} \int_0^\infty d\tau \\ \times \exp[ix\tau - \tau - i^{\frac{1}{2}} \Gamma(\frac{1}{4}) \alpha \tau^{\frac{1}{2}}]. \quad (4.11)$$

This is not the exact quasi-static theory result, because in this limit the assumption of scalar additivity is not valid, and also because of the difficulty with the magnetic quantum numbers. However, as was indicated, this does not lead to serious errors. The correct quasi-static approximation is obtained by averaging the impact profiles over the static shifts due to the instantaneous ion field, using the proper statistical distribution function

$$I_H(\omega) = \frac{w}{\pi} \int_0^\infty \frac{W(F) dF}{w^2 + [\omega - d - (2\pi/e^2) C_4 F^2]^2}, \quad (4.12)$$

<sup>25</sup> The derivation follows again reference 5. A useful integral,

$$\int_0^\infty \frac{dx}{x^{1+\sigma}} (1 - e^{-ix}) = \frac{\pi}{\sin \pi \sigma} \frac{e^{i\pi\sigma/2}}{\Gamma(1+\sigma)},$$

is obtained from H. Jensen, Z. Physik **80**, 448 (1933).



which gives, with the Holtsmark distribution function,

$$W_H(\beta) = W_H(F/F_0) = F_0 W(F),$$

$$F_0 = 2.61eN^{\frac{1}{2}},$$

$$(2\pi/e^2)C_4F_0^2 = \omega\alpha^{\frac{1}{2}},$$

$$I_H(\omega) = -\frac{\omega}{\pi} \int_0^\infty \frac{W_H(\beta)d\beta}{\omega^2 + (\omega - d - \omega\alpha^{\frac{1}{2}}\beta^2)^2},$$
(4.13)

and

$$j_H(x, \alpha) = -\frac{1}{\pi} \int_0^\infty \frac{W_H(\beta)d\beta}{1 + (x - \alpha^{\frac{1}{2}}\beta^2)^2},$$
(4.14)

or finally in dimensionless variables

As indicated in Appendix Z, Eqs. (4.9), (4.11), and (4.14) reduce to the asymptotic wing formulas for large  $x$ . This is as expected, because then both the quasi-static and the nearest-neighbor approximations are valid for ions, and the distinction between scalar or vector addition of the individual ion fields is accordingly irrelevant.

For large ion velocities one has the phase shift limit<sup>26,27</sup> (see, e.g., reference 11)

$$\lim_{\sigma \rightarrow 0} j(x, \alpha, \sigma) = -\frac{1}{\pi} \operatorname{Re} \int_0^\infty d\tau$$

$$\times \exp[i x \tau - i^{\frac{3}{4}} \frac{\pi}{2} \Gamma(\frac{1}{3}) \alpha^{8/9} \sigma^{-\frac{1}{3}} \tau],$$
(4.15)

i.e., a dispersion profile whose width in units of the electron width (in the  $x$  scale) is

$$w_x = 1 + \frac{\pi}{8} \Gamma(\frac{1}{3}) \alpha^{8/9} \sigma^{-\frac{1}{3}} = 1 + 1.36 \alpha^{8/9} \sigma^{-\frac{1}{3}},$$
(4.16)

and whose shift due to ions, also in the  $x$  scale, is

$$d_x = \pm (3\sqrt{3}/8) \Gamma(\frac{1}{3}) \alpha^{8/9} \sigma^{-\frac{1}{3}}$$

$$= \pm 2.36 \alpha^{8/9} \sigma^{-\frac{1}{3}}.$$
(4.17)

(The sign is determined by that of  $\alpha$  and  $C_4$ .)

Debye shielding of ion fields by electrons and ion-ion correlations are much less important for the neutral helium lines considered in this section than for hydrogen lines. First of all, because of the second-order Stark effect, only relatively large ion field strengths are of interest, whose probability is not much affected by correlations and shielding. In addition, at high densities where these effects might be of interest, helium lines can only be observed at much higher temperatures than hydrogen lines. Finally, the ions contribute here a much smaller part of the broadening, so that neglecting the two effects is not expected to reduce the accuracy of the theoretical profiles significantly except, perhaps, near the intensity maxima.

<sup>26</sup> E. Lindholm, Arkiv. mat. astron. Fysik **28B**, No. 3 (1941) and dissertation, Uppsala, 1942 (unpublished).

<sup>27</sup> H. M. Foley, Phys. Rev. **69**, 616 (1946).

## 5. FORBIDDEN LINES

If the splitting between neighboring levels is of the same order as the corresponding  $\phi$ -matrix elements, or if the instantaneous shifts due to the ions are of similar magnitude, forbidden components will be excited. In the neighborhood of a forbidden component denoted by  $i$  and after expansion and normalization, Eq. (2.10) becomes

$$I_i^{e1}(\omega) = \frac{-\phi_{ii}}{\pi} (\omega_i^2 + \phi_{ii}^2)^{-1} \left( \left| \frac{\mu_i}{\mu_0} \right|^2 - \left| \frac{\phi_{i0}}{\omega_{i0}} \right|^2 + \frac{2 \operatorname{Re}(\mu_0 \mu_i^* \phi_{i0} \omega_i)}{|\mu_0|^2 \phi_{ii} \omega_{i0}} \right),$$
(5.1)

with the abbreviations

$$\langle \beta | \mu_\sigma | \alpha^{(i)} \rangle \equiv \mu_i, \quad \langle \alpha^{(i)} | \phi | \alpha^{(k)} \rangle \equiv \phi_{ik},$$

$$\omega_i \equiv \omega - \langle \alpha^{(i)} | H_{0a} | \alpha^{(i)} \rangle - \langle \beta | H_{0b} | \beta \rangle / \hbar,$$

$$\omega_{i0} = \omega_i - \omega_0.$$
(5.2)

Eq. (5.1) holds for  $|\omega_i| \ll |\omega_0|$ , i.e., in the neighborhood of the forbidden component. The contribution of the allowed component ( $i=0$ ) is not included here and it was assumed that the forbidden line is weak compared to the allowed line ( $|\mu_0| \gg |\mu_i|$ ,  $|\omega_{i0}| \gg |\phi_{i0}|$ ) and that all  $\phi$ -matrix elements are real. The latter assumption is not a serious restriction because forbidden components only appear at high densities, where the hydrogenic approximation for the  $\phi$  matrix is applicable.

The ion effects on such lines can be calculated using the quasi-static theory, which is generally valid at high densities. The hydrogenic  $\phi$  matrix and  $\mu_0$  are practically independent of the ion field strength in the case considered here, and the observable profile of a forbidden line is therefore

$$I_i(\omega) = \int dF W(F) I_i^{e1}(\omega)$$

$$= \frac{-\phi_{ii}}{\pi} \int \frac{dF W(F)}{\omega_i^2(F) + \phi_{ii}^2} \left( \left| \frac{\mu_i(F)}{\mu_0} \right|^2 - \left| \frac{\phi_{i0}}{\omega_{i0}(F)} \right|^2 + \frac{2 \operatorname{Re}[\mu_0 \mu_i^*(F)] \phi_{i0} \omega_i(F)}{|\mu_0|^2 \phi_{ii} \omega_{i0}(F)} \right).$$
(5.3)

If several forbidden components exist, they will usually be so closely spaced that they show a linear Stark effect. Then the components shifted towards the allowed line will be the most important, and  $I_i^{e1}(\omega)$  in the integrand of (5.3) will increase rapidly with field strength until all components merge at a maximum field strength  $F_{\max}$  given by

$$|eF_{\max} z_{0i}| \approx |\hbar \omega_{i0}(0)|$$
(5.4)

(with  $z_{0i} \equiv \langle \alpha^{(0)} | z | \alpha^{(i)} \rangle$ ).

The quantity which is most critically affected by the ion field is  $|\mu_i(F)/\mu_0|^2$ , whose mean value can be esti-

mated using the asymptotic Holtsmark distribution

$$W_{\text{as}}(\bar{F}) = 2\pi e^{\frac{3}{2}} N \bar{F}^{-\frac{3}{2}}, \quad (5.5)$$

Eq. (5.4), and the standard quadratic Stark effect result,

$$\begin{aligned} \left\langle \left| \frac{\mu_i(F)}{\mu_0} \right|^2 \right\rangle_{\text{av}} &\approx \int_0^{F_{\text{max}}} dFW(F) \left| \frac{ez_{0i}F}{\hbar\omega_{i0}(0)} \right|^2 \\ &= 4\pi e^{\frac{3}{2}} N \left| \frac{z_{0i}}{\hbar\omega_{i0}(0)} \right|^{\frac{3}{2}}. \end{aligned} \quad (5.6)$$

For densities at which the forbidden components are sufficiently weak, the maximum field strength is always much larger than the mean field strength

$$\bar{F} = 8.8eN^{\frac{2}{3}}. \quad (5.7)$$

Therefore, the probability of fields greater than  $F_{\text{max}}$  which produce a linear Stark effect in the allowed component is very small, so that the cutoff in the above integral is not critical.

The mean values of the other relevant quantities, now assuming linear Stark effect and neglecting the shift of the allowed line, are

$$\begin{aligned} \langle \omega_i(F) \rangle_{\text{av}} &= \omega_i(0) + \hbar^{-1} ez_{ii} \bar{F}, \\ \langle \omega_{i0}(F) \rangle_{\text{av}} &= \omega_{i0}(0) + \hbar^{-1} ez_{ii} \bar{F}, \\ \frac{\text{Re}(\mu_0 \mu_i(F))_{\text{av}}}{|\mu_0|^2} &= \frac{ez_{0i} \bar{F}}{\hbar\omega_{i0}(0)}. \end{aligned} \quad (5.8)$$

Using these relations and (5.7) for  $N$ , (5.3) may finally be approximated by

$$\begin{aligned} I_i(\omega) &\approx \frac{-\phi_{ii}}{\pi} \{ [\omega_i(0) + \hbar^{-1} ez_{ii} \bar{F}]^2 + \phi_{ii}^2 \}^{-1} \\ &\times \left[ 4\pi \left| \frac{ez_{0i} \bar{F}}{8.8\hbar\omega_{i0}(0)} \right|^{\frac{3}{2}} - \left| \frac{\phi_{i0}}{\omega_{i0}(0) + \hbar^{-1} ez_{ii} \bar{F}} \right|^2 \right. \\ &\quad \left. + \frac{2ez_{0i} \bar{F} \phi_{i0} [\omega_i(0) + \hbar^{-1} ez_{ii} \bar{F}]}{\hbar\omega_{i0}(0) \phi_{ii} [\omega_{i0}(0) + \hbar^{-1} ez_{ii} \bar{F}]} \right]. \end{aligned} \quad (5.9)$$

(The strongest forbidden component will be that for which  $\omega_{i0}(0)$  and  $ez_{ii} \bar{F} / \hbar$  have different signs.) Hydrogen wave functions can be used for all the matrix elements with adequate accuracy or—for the forbidden components showing a linear Stark effect—the linear combinations which diagonalize the  $z$  matrix.

The last term in (5.9) will often be negligible. Then one can say that the first term represents the excitation of the forbidden components by the quasi-static action of the ions, and the second term represents their de-excitation by electron impacts. The second term increases somewhat faster with the electron density than the first term, i.e., electron effects become more and more important at high densities.

When the intensities of the forbidden lines approach that of the allowed lines, the approximations made in this section are no longer valid. For example, the profile of the HeI 3965A line was computed<sup>28</sup> using the complete impact profile described by Eq. (2.10), folded into the ion field-strength distribution, and the result agreed with Wulff's experiment<sup>29</sup> within  $\sim 20\%$ . [These calculations were made for the electron density  $3.2 \times 10^{16} \text{ cm}^{-3}$  quoted by Wulff, but only one interacting state was considered in the  $\phi$ -matrix elements. New calculations with more interacting states (up to five) give best agreement for an electron density  $2.5 \times 10^{16} \text{ cm}^{-3}$ .] In this case the forbidden component has practically always a linear Stark effect, and for high field strengths also the allowed component. If this transition to linear Stark effect occurs already for relatively small field strength, the theory developed for hydrogen lines<sup>3</sup> must be applied, and the profile will correspond to that of a hydrogen line with the same upper state, except for trivial factors due to the difference in wavelengths and the fact that usually the  $S$  states do not merge.

## 6. NUMERICAL RESULTS AND USE OF TABLES

The electron impact widths and shifts using Eqs. (3.15) and (3.16) were calculated with an IBM-704 computer. Broadening and shift of both the upper and lower states were taken into account with a maximum of five interacting states by adding the widths and subtracting the shifts of upper and lower states. Also calculated were the parameters  $\alpha$  and  $\sigma$  [see Eq. (4.8)], which characterize the ion broadening. (For  $\sigma$  the mean value of  $v^{\frac{3}{2}}$  was employed, assuming electron and ion kinetic temperatures to be the same.) All quantities are tabulated (Table I) for electron densities  $N'$  which were chosen to be smaller than the densities for which the various allowed lines overlap. (These  $N'$  are almost always smaller than  $N_{\text{max}}$  defined by (3.19), i.e., Debye shielding is usually negligible in the electron broadening.) For electron densities  $N$  smaller than  $N'$  the widths of lines without forbidden components are obtained by multiplying the tabulated values with  $N/N'$ , the asymmetry parameters  $\alpha$  by multiplying with  $(N/N')^{\frac{1}{2}}$  and the parameters  $\sigma$  by multiplying with  $(N/N')^{\frac{3}{2}}$ . If other than helium ions dominate the ion broadening,  $\sigma$  must be multiplied by the square root of the foreign ion to helium mass ratio. The electron impact shifts follow directly from the tabulated shift-width ratios, which are positive if the line has a red shift. Also given for comparison is the adiabatic theory result for the widths.

For many cases, the linewidths obtained with the adiabatic approximation are not too different from those derived from the generalized impact theory, but

<sup>28</sup> H. R. Griem and A. C. Kolb, *Proceedings of the Fourth International Conference on Ionization Phenomena in Gases*, Uppsala, Sweden, August 17–21, 1959 (North-Holland Publishing Company, Amsterdam, 1960).

<sup>29</sup> H. Wulff, *Z. Physik* **150**, 614 (1958).

TABLE I. Calculated line broadening parameters: electron impact (half) half-widths  $w$ , adiabatic widths  $w'$ , relative shifts  $d/w$ , and ion broadening parameters  $\alpha$  and  $\log_{10}\sigma$ . [The widths are in Å for electron densities  $N'$  in  $\text{cm}^{-3}$  and the static Stark coefficients  $C$  and  $C'$  are in units of  $\text{cm}^{-1}$  per  $(100 \text{ kv/cm})^2$ .]

Line \ T [°K]	5000	10 000	20 000	40 000	80 000
$1^1S-4^1P$	$w$ 1.91	1.78	1.60	1.40	1.18
522.2Å	$w'$ 1.76	1.97	2.22	2.49	2.80
$N'=10^{18}$	$d/w$ -0.64	-0.54	-0.44	-0.36	-0.30
$C=+39.4$	$\alpha$ 0.84	0.89	0.96	1.06	1.21
	$\log\sigma$ 2.23	2.05	1.86	1.65	1.42
$1^1S-3^1P$	$w$ 0.458	0.433	0.398	0.356	0.308
537.1Å	$w'$ 0.412	0.462	0.519	0.582	0.654
$N'=10^{18}$	$d/w$ -0.67	-0.55	-0.44	-0.35	-0.28
$C=+4.10$	$\alpha$ 0.47	0.49	0.52	0.57	0.63
	$\log\sigma$ 1.59	1.41	1.23	1.03	0.81
$1^1S-2^1P$	$w$ 1.21	1.62	2.03	2.36	2.52
584.4Å	$w'$ 0.53	0.59	0.66	0.74	0.83
$N'=10^{20}$	$d/w$ -0.65	-0.28	-0.04	+0.08	+0.12
$C=+0.0046$	$\alpha$ 0.16	0.13	0.11	0.10	0.09
	$\log\sigma$ 1.27	1.25	1.19	1.11	0.98
$2^3S-4^3P$	$w$ 33.2	35.8	36.2	34.7	31.7
3188Å	$w'$ 20.4	22.9	25.7	28.8	32.4
$N'=10^{18}$	$d/w$ +0.70	+0.49	+0.36	+0.27	+0.21
$C=-6.83$	$\alpha$ 0.40	0.38	0.38	0.39	0.41
$C'=-6.2$	$\log\sigma$ 1.90	1.78	1.64	1.47	1.28
$2^3S-3^3P$	$w$ 10.6	11.7	12.3	12.2	11.7
3889Å	$w'$ 6.44	7.23	8.12	9.11	10.2
$N'=10^{18}$	$d/w$ +0.73	+0.50	+0.34	+0.24	+0.17
$C=-0.67$	$\alpha$ 0.22	0.21	0.20	0.20	0.21
$C'=-0.71$	$\log\sigma$ 1.23	1.13	0.99	0.84	0.67
$2^1S-4^1P$	$w$ 110	102	92.5	80.9	68.2
3965Å	$w'$ 102	114	128	144	161
$N'=10^{18}$	$d/w$ -0.65	-0.54	-0.45	-0.37	-0.31
$C=+39.4$	$\alpha$ 0.84	0.89	0.96	1.06	1.21
$C'=+37.3$	$\log\sigma$ 2.23	2.05	1.86	1.65	1.42
$2^3P-5^3S$	$w$ 82.9	98.4	108	111	105
4121Å	$w'$ 59.4	66.7	74.8	84.0	94.3
$N'=10^{18}$	$d/w$ +1.38	+1.14	+0.91	+0.73	+0.59
$C=-15.7$	$\alpha$ 0.55	0.49	0.45	0.45	0.46
	$\log\sigma$ 2.08	2.00	1.89	1.75	1.58
$2^1P-5^1S$	$w$ 148	168	176	172	158
4438Å	$w'$ 101	114	128	143	161
$N'=10^{18}$	$d/w$ +1.23	+0.99	+0.79	+0.64	+0.52
$C=-28.1$	$\alpha$ 0.62	0.56	0.54	0.55	0.59
	$\log\sigma$ 2.26	2.17	2.04	1.88	1.69
$2^3P-4^3S$	$w$ 35.5	43.0	49.0	51.9	51.2
4713Å	$w'$ 26.6	29.8	33.5	37.6	42.2
$N'=10^{18}$	$d/w$ +1.49	+1.25	+1.02	+0.82	+0.66
$C=-3.14$	$\alpha$ 0.38	0.33	0.30	0.28	0.29
$C'=-2.9$	$\log\sigma$ 1.59	1.52	1.43	1.30	1.15
$2^1S-3^1P$	$w$ 40.1	37.9	35.2	31.9	28.0
5016Å	$w'$ 36.1	40.6	45.5	51.1	57.4
$N'=10^{18}$	$d/w$ -0.69	-0.58	-0.49	-0.40	-0.33
$C=+4.14$	$\alpha$ 0.47	0.49	0.52	0.56	0.62
$C'=+4.3$	$\log\sigma$ 1.59	1.41	1.23	1.04	0.83
$2^1P-4^1S$	$w$ 65.0	75.5	81.7	82.3	77.9
5048Å	$w'$ 45.8	51.4	57.7	64.8	72.8
$N'=10^{18}$	$d/w$ +1.32	+1.09	+0.88	+0.71	+0.58
$C=-5.79$	$\alpha$ 0.43	0.38	0.36	0.36	0.37
$C'=-5.2$	$\log\sigma$ 1.79	1.71	1.59	1.44	1.27
$2^3P-3^3D$	$w$ 16.5	17.6	18.1	18.0	17.3
5876Å	$w'$ 10.2	11.5	12.9	14.4	16.2
$N'=10^{18}$	$d/w$ -0.60	-0.33	-0.13	-0.02	+0.03
$C=+0.39$	$\alpha$ 0.20	0.19	0.18	0.18	0.19
$C'=+0.67$	$\log\sigma$ 1.07	0.94	0.81	0.65	0.48

TABLE I (continued).

Line	T [°K]	5000	10 000	20 000	40 000	80 000
2 <sup>1</sup> P-3 <sup>1</sup> D	w	44.6	40.5	36.6	32.9	29.0
6678A	w'	44.9	50.4	56.5	63.5	71.3
N' = 10 <sup>18</sup>	d/w	+0.65	+0.60	+0.56	+0.51	+0.45
C = -2.43	α	0.45	0.48	0.52	0.56	0.62
C' = -2.6	logσ	1.39	1.19	1.00	0.80	0.60
2 <sup>3</sup> P-3 <sup>3</sup> S	w	18.2	22.5	26.5	29.3	30.3
7065A	w'	14.4	16.1	18.1	20.3	22.8
N' = 10 <sup>18</sup>	d/w	+1.59	+1.37	+1.14	+0.91	+0.72
C = -0.37	α	0.23	0.20	0.18	0.16	0.16
C' = -0.25	logσ	0.95	0.89	0.81	0.70	0.57
2 <sup>1</sup> P-3 <sup>1</sup> S	w	32.5	38.9	43.6	45.8	44.9
7281A	w'	23.9	26.8	30.0	33.7	37.9
N' = 10 <sup>18</sup>	d/w	+1.43	+1.20	+0.98	+0.78	+0.63
C = -0.72	α	0.26	0.23	0.21	0.20	0.21
	logσ	1.17	1.10	1.00	0.87	0.71
3 <sup>3</sup> P-5 <sup>3</sup> S	w	80.8	97.3	109	112	108
12 850A	w'	56.0	62.9	70.5	79.2	89.0
N' = 10 <sup>17</sup>	d/w	+1.33	+1.07	+0.85	+0.67	+0.54
C = -15.0	α	0.30	0.26	0.24	0.23	0.24
	logσ	1.42	1.34	1.24	1.10	0.93
3 <sup>1</sup> P-5 <sup>1</sup> S	w	147	166	174	170	157
13 477A	w'	102	114	128	145	163
N' = 10 <sup>17</sup>	d/w	+1.21	+0.99	+0.79	+0.64	+0.52
C = -32.2	α	0.36	0.33	0.32	0.33	0.35
	logσ	1.63	1.53	1.40	1.24	1.05
3 <sup>1</sup> S-4 <sup>1</sup> P	w	161	152	140	125	108
15 088A	w'	149	167	187	210	236
N' = 10 <sup>17</sup>	d/w	-0.70	-0.60	-0.52	-0.44	-0.37
C = +40.1	α	0.48	0.50	0.53	0.57	0.64
	logσ	1.57	1.39	1.21	1.01	0.79
3 <sup>1</sup> D-4 <sup>1</sup> P	w	257	240	218	191	162
18 561A	w'	231	260	291	327	367
N' = 10 <sup>17</sup>	d/w	-0.66	-0.56	-0.46	-0.39	-0.33
C = +41.8	α	0.47	0.50	0.53	0.59	0.67
	logσ	1.59	1.41	1.22	1.01	0.79
3 <sup>3</sup> D-4 <sup>3</sup> P	w	129	140	143	139	128
19 548A	w'	79.6	89.3	100	113	126
N' = 10 <sup>17</sup>	d/w	+0.75	+0.53	+0.38	+0.28	+0.21
C = -7.23	α	0.23	0.22	0.21	0.22	0.23
	logσ	1.25	1.13	0.99	0.83	0.64
3 <sup>3</sup> P-4 <sup>3</sup> S	w	75.4	95.8	112	121	121
21 127A	w'	45.4	51.0	57.2	64.2	72.1
N' = 10 <sup>17</sup>	d/w	+1.18	+0.96	+0.78	+0.62	+0.50
C = -2.48	α	0.17	0.14	0.13	0.12	0.12
	logσ	0.95	0.90	0.82	0.70	0.55
3 <sup>1</sup> P-4 <sup>1</sup> S	w	152	170	179	178	168
21 138A	w'	115	129	144	162	182
N' = 10 <sup>17</sup>	d/w	+1.20	+1.01	+0.83	+0.67	+0.55
C = -9.9	α	0.29	0.27	0.25	0.25	0.27
	logσ	1.25	1.15	1.02	0.87	0.69
4 <sup>1</sup> P-5 <sup>1</sup> S	w	252	269	273	262	239
46 066A	w'	196	220	247	277	311
N' = 10 <sup>16</sup>	d/w	+1.07	+0.89	+0.73	+0.59	+0.49
C = -67.5	α	0.27	0.25	0.25	0.26	0.28
	logσ	1.13	1.00	0.86	0.69	0.50
4 <sup>3</sup> P-5 <sup>3</sup> S	w	128	159	181	188	182
46 950A	w'	52.6	59.0	66.2	74.3	83.6
N' = 10 <sup>16</sup>	d/w	+0.81	+0.67	+0.55	+0.44	+0.36
C = -8.9	α	0.10	0.08	0.08	0.08	0.08
	logσ	0.82	0.76	0.67	0.53	0.37

deviations by a factor of 2 or 3 in both directions occur occasionally. The adiabatic widths increase monotonically with temperature, while the widths calculated here often have a maximum for intermediate temperatures, so that their temperature dependence is even smaller than the  $T^{1/6}$  dependence in the adiabatic approximation. It is for this reason that densities can be determined when the temperature is not known precisely and even when one is not sure about the existence of local equilibrium. The ratios of shifts and widths are always smaller than the adiabatic theory result  $\sqrt{3}$ , usually by a factor of 2 or more, especially at higher temperatures.

In the first column of Table I the calculated and the available measured<sup>30</sup> values (averaged over the polarizations) of the quadratic Stark effect coefficients  $C$  and  $C'$  are compared to provide a check on the accuracy of the atomic wave functions used in the line broadening calculations. The agreement is usually within 10%. This error causes slightly smaller uncertainties in the linewidths and shifts.

That errors of this order must be expected can also be seen from Table II, where atomic matrix elements obtained from various approximations are given. Hartree-Fock calculations<sup>31</sup> were only available for states with principal quantum number 2. For higher states, hydrogen-like wave functions had to be used, in which either the charge or the principal quantum number<sup>32</sup> was adjusted to give the measured bound state energies. Matrix elements involving states with different principal quantum numbers given only a small contribution to the line broadening so that they could be approximated by the hydrogenic values.

In Table III the reduced line profiles  $j(x, \alpha, \sigma)$  (time-dependent ion fields) and  $j_H(x, \alpha)$  (quasi-static ion fields) from Eqs. (4.9) and (4.14) are presented for all values of  $\alpha$  and  $\sigma$  of interest. If  $\sigma$  is larger than the

TABLE II. Squares of radial matrix elements in atomic units for the singlet (in parentheses) and the triplet system of neutral helium calculated with various approximations.

	Hartree-Fock	Effect. quantum number	Effect. charge	Hydrogen	Adopted value
$\langle(2S r 2P)\rangle^2$	21.03 (25.56)	19.32 (25.22)	23.55 (26.16)	27	21.0 (25.6)
$\langle(3S r 3P)\rangle^2$		125.2 (152.0)	146.4 (158.5)	162	134 (154)
$\langle(3P r 3D)\rangle^2$		102.7 (100.0)	101.7 (100.9)	101.25	101 (101)
$\langle(4S r 4P)\rangle^2$		432.2 (505.8)	498.4 (529.8)	540	459 (514)
$\langle(4P r 4D)\rangle^2$		435.9 (428.1)	433.0 (437.8)	432	432 (432)
$\langle(5S r 5P)\rangle^2$		1103 (1270)	1263 (1328)	1350	1170 (1290)

largest tabulated value  $\sigma_{\max}$ , then  $j_H(x, \alpha)$  can be used; and if  $\sigma$  is smaller than the smallest tabulated values, the impact approximation becomes applicable for ions, i.e., Eqs. (4.16) and (4.17) may be used to evaluate the total width and shift of the resulting dispersion profile. For larger  $x$  values than those in the table, the wing formulas derived in Appendix Z can be employed, i.e., Eqs. (Z10) or (Z11) and (Z12).

At low densities ion broadening is only important on the line wings, where the scalar additivity assumption is not critical. At high densities the whole profile is seriously affected, but  $j_H(x, \alpha)$  can then be applied which makes use of the quasi-static approximation for the ions without the assumption of binary collisions and scalar additivity. In order to show that the quasi-static assumption causes no significant errors for larger  $\sigma$  values, the function  $j(x, \alpha, \infty)$  [from (4.11)] is also tabulated in Table III. It deviates from both  $j(x, \alpha, \sigma_{\max})$  and  $j_H(x, \alpha)$  by less than  $\sim 10\%$  for  $\alpha < 0.3$ , which may be taken as an indication of the errors in the complete line profiles due to the scalar additivity approximation made in the calculation of the time-dependent ion

TABLE III. Reduced line profiles  $j(x, \alpha, \sigma)$  and  $j_H(x, \alpha)$  for various values of the ion broadening parameters  $\alpha$  and  $\sigma$ .

$\alpha \setminus \frac{x}{\sigma}$	-2.0	-1.5	-1.0	-0.7	-0.5	-0.3	-0.2	-0.1	0.0	0.1	0.2	0.3	0.5	0.7	1.0	1.5	2.0	2.5	3.0	4.0	5.0	
0.1	1.0	0.052	0.073	0.111	0.148	0.173	0.200	0.214	0.226	0.239	0.251	0.259	0.265	0.261	0.242	0.204	0.142	0.096				
	$\infty$	0.049	0.072	0.114	0.153	0.186	0.221	0.238	0.254	0.267	0.277	0.282	0.283	0.270	0.244	0.199	0.132	0.089				
	$j_H$	0.050	0.073	0.115	0.154	0.186	0.218	0.235	0.247	0.260	0.270	0.274	0.274	0.263	0.240	0.198	0.134	0.092				
0.2	0.6	0.044	0.058	0.083	0.103	0.121	0.141	0.150	0.161	0.172	0.182	0.194	0.204	0.219	0.223	0.211	0.171	0.127				
	1.0	0.039	0.056	0.084	0.110	0.130	0.153	0.166	0.180	0.193	0.205	0.217	0.227	0.238	0.231	0.215	0.167	0.121				
	$\infty$	0.038	0.054	0.083	0.110	0.134	0.162	0.177	0.195	0.207	0.222	0.234	0.243	0.253	0.248	0.221	0.163	0.115				
	$j_H$	0.039	0.056	0.088	0.116	0.143	0.169	0.183	0.196	0.208	0.220	0.228	0.234	0.238	0.228	0.206	0.156	0.114				
0.3	0.3	0.041	0.055	0.075	0.091	0.105	0.122	0.130	0.139	0.147	0.155	0.162	0.171	0.186	0.199	0.212	0.206	0.166				
	0.6	0.036	0.049	0.071	0.089	0.104	0.121	0.130	0.139	0.149	0.158	0.167	0.175	0.192	0.207	0.219	0.198	0.158				
	1.0	0.032	0.045	0.067	0.087	0.103	0.123	0.133	0.144	0.155	0.163	0.172	0.183	0.201	0.214	0.218	0.190	0.145				
	$\infty$	0.030	0.042	0.062	0.082	0.098	0.118	0.130	0.142	0.154	0.170	0.183	0.195	0.214	0.225	0.222	0.184	0.139				
	$j_H$	0.032	0.045	0.069	0.091	0.109	0.131	0.143	0.155	0.166	0.178	0.188	0.195	0.204	0.206	0.197	0.164	0.128	0.100	0.078	0.047	0.030
0.4	$j_H$	0.026	0.038	0.056	0.073	0.086	0.104	0.113	0.123	0.131	0.141	0.150	0.157	0.170	0.175	0.176	0.160	0.134	0.110	0.090	0.058	0.036
0.5	$j_H$	0.022	0.032	0.047	0.058	0.072	0.090	0.094	0.102	0.110	0.117	0.127	0.133	0.144	0.154	0.156	0.148	0.130	0.113	0.096	0.065	0.040

<sup>30</sup> Landolt-Börnstein, *Zahlenwerte und Funktionen I.1* (Springer-Verlag, Berlin, 1950).

<sup>31</sup> E. Treffitz, A. Schüter, K. H. Dettmar, and K. Jörgens, *Z. Astrophys.* 44, 1 (1957).

<sup>32</sup> D. R. Bates and A. Damgaard, *Phil. Trans. Roy. Soc. London A242*, 10 (1942).

TABLE IV. Analysis of the arc experiment.

Wavelength [Å]	Half-width $w$ [Å]		Shift $d$ [Å]		Electron density $N$ [ $10^{16}$ cm $^{-3}$ ]		
	measured	calculated	measured	calculated	$N_{\text{ex}}$	$N_{\text{ex}'}$	$N_{\text{ex}''}$
3889	0.37	0.34	0.25	0.15	2.7	4.3	3.5
5016	0.91	0.99	0.65	0.73	2.3	1.9	1.6
4713	1.5	1.4	1.5	1.4	2.6	4.2	3.4
4121	3.1	3.3	2.8	3.0	2.4	3.9	3.2
5048	2.3	2.3	2.1	2.3	2.5	3.7	3.0

broadening. [For  $\alpha > 0.3$ , one can practically always use  $j_H(x, \alpha)$ .]

Line profiles on an absolute wavelength scale can be obtained from the reduced profiles by multiplying the  $x$  values with the electron impact width  $w$ , dividing the intensities by  $w$ , and finally shifting the whole profile by the electron impact shift  $d$ . A numerical accuracy close to 20% is expected for all the lines listed in Table I, if the densities are below  $N'$ , and if forbidden components are treated as indicated in the preceding section. The schematic treatment of close electron collisions, the uncertainties in the wave functions, and the approximations in the treatment of the ions contribute comparable amounts to this error.

## 7. COMPARISON WITH EXPERIMENT

Measurements of profiles of neutral helium lines have been made with pulsed arcs<sup>29</sup> and with explosive-driven shock tubes.<sup>33</sup> In the arc experiment the electron density could be estimated from the volume and initial pressure, and the temperature was measured to be  $T = 30\,000^\circ\text{K}$

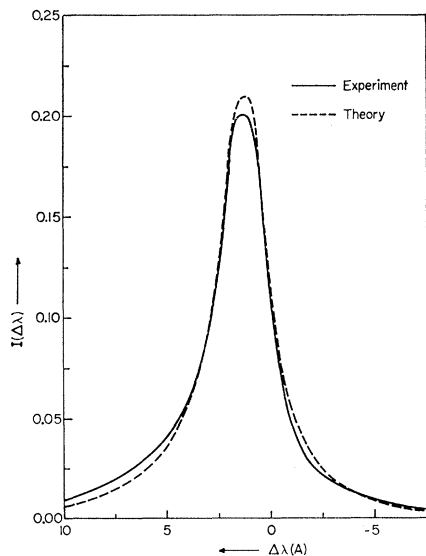


FIG. 3. Profile of the HeII 4713A line at  $N = 2.5 \times 10^{16}$  cm $^{-3}$  and  $T = 30\,000^\circ\text{K}$ .

<sup>33</sup> G. E. Seay, Los Alamos Scientific Laboratory Report LAMS-2125, 1957 (unpublished).

from the relative intensities of the HeII 4686 Å and the HeI 4713 Å lines, using the value for the electron density.

Table IV summarizes the results of the arc experiment for five isolated lines. The second and fourth columns give the measured half-widths and shifts. From the measured widths the corresponding electron densities  $N_{\text{ex}}$  (column 6) were computed from the present theory taking into account both ions and electrons. This was done by an iteration procedure where the ions were neglected as a first approximation. For comparison, the densities  $N_{\text{ex}'}$  obtained from the adiabatic theory for electron broadening neglecting the ions are listed in column 7. In column 8 the density  $N_{\text{ex}''}$  obtained from the adiabatic impact approximation for both ions and electrons is given. It can be seen that the densities determined from the present theory only deviate by  $\pm 10\%$  from their mean value of  $2.5 \times 10^{16}$  cm $^{-3}$ , i.e., are consistent with each other within the errors of theory and experiment. (The densities obtained from the adiabatic approximation show deviations of up to a factor of 1.5 from their mean value.) The shift was then computed for this new density and agrees within the experimental accuracy with the measured shifts. It should be noted that the ratio of the shift to width is considerably smaller than the adiabatic prediction of  $\sqrt{3}$ . For completeness the half-widths are computed for  $N = 2.5 \times 10^{16}$  cm $^{-3}$  and tabulated in column 3.

The  $N_{\text{ex}}$  from this theory are smaller than the originally quoted<sup>29</sup> electron density  $N = 3.2 \times 10^{16}$  cm $^{-3}$ . This is consistent with the measured profile of the HeII 4686 Å line which also corresponds to a smaller electron density if electron broadening is not neglected.<sup>6</sup>

Complete profiles of one isolated line and one line with a forbidden component were calculated for  $N = 2.5 \times 10^{16}$  cm $^{-3}$  and  $T = 30\,000^\circ\text{K}$ , and are compared with Wulff's measured profiles in Figs. 3 and 4 without translation of the wavelength scale, i.e., the shift was calculated. The agreement is again as good as can be expected, even for the forbidden component in the second example. The deviation on the line wings may be due to errors in the determination of the continuum background. No attempt was made to show profiles from previous theories, because they disagree with the measured profiles far outside the experimental error.

The shock-tube data of Seay<sup>33</sup> also show large dis-

crepancies between the observed helium profiles and those calculated from the usual adiabatic theories, particularly in the shifts which are smaller than expected from the Lindholm-Foley analysis.<sup>26,27</sup> Because of experimental difficulties associated with uncertainties due to the time resolution and self-absorption, the shock-tube measurements at the present time are not as accurate as the arc data. However, with improved time resolution and with independent density measurements (from the continuum, the broadening of hydrogenic lines, interferometric determinations,<sup>34</sup> and shock velocities), the shock tube holds promise of a spectroscopic precision comparable to that of the pulsed arc (which burns for milliseconds compared with the microsecond time scale of the shock-tube experiments) because the errors due to the short time scale can be less than those due to spatial inhomogeneities in arcs. Because of these spatial inhomogeneities it is unlikely that the measured widths, shifts, and electron densities in the arc are accurate to better than 20%, whereas the accuracy in recent measurements of hydrogen and neutral and ionized helium line profiles with electromagnetic shock tubes<sup>35</sup> seems to be at least twice as good as far as the widths are concerned.

8. RELATIONSHIP WITH EARLIER THEORIES

The comparison of the present work with the usual Lindholm-Foley<sup>26,27</sup> adiabatic theory of electron broadening has already been discussed in Sections 3 and 6.

A theory of the electron width has been given by Rudkjöbing.<sup>36</sup> It is an impact theory, but he considers only collisions where the electrons are scattered elastically by the Hartree potential of the atom. Hence his widths are much too small since, as was seen in Sec. 3, the greater part of the width usually comes from inelastic collisions. Even for elastic collisions alone, his is an underestimate due to his neglect of polarization.

For some years, a standard work on helium lines has been that of Kivel.<sup>37</sup> His width includes only inelastic collisions and is given by  $w = \frac{1}{2} N v \sigma_i$ , where  $\sigma_i$  is the total electron inelastic cross section computed with the quantum mechanical Born approximation. This should be correct if the Born approximation is valid. The use of the Born approximation is equivalent to the use of perturbation theory in Sec. 3 for calculating  $\phi_a$ . It is not valid for small impact parameters, hence the introduction in Sec. 3 of  $\rho_{min}$  and its definition by Eq. (3.16). Kivel's width is obtained from (3.15) by setting  $\rho_{min}$  equal to  $\lambda$ , the de Broglie wavelength divided by  $2\pi$ , the explanation being that the main effect of quantum mechanics is to quantize the angular momentum of

the electron, thus making impact parameters smaller than  $\lambda$  meaningless. If  $\rho_{min}$  as defined by Eq. (3.16) turns out to be much smaller than  $\lambda$ , the classical path theory is wrong and Kivel's width should be used. If  $\rho_{min}$  is of order  $\lambda$ , both theories give the same result. And if  $\rho_{min}$  is much larger than  $\lambda$ , Kivel's use of the Born approximation is improper and Eqs. (3.15)–(3.16) should be used. For neutral atoms, it turns out that  $\rho_{min}$  is always larger than  $\lambda$  in the high-velocity limit, as shown by Eq. (3.13), and also in the adiabatic limit if the perturber energies are larger than the energy differences of interacting levels. Hence the classical path theory is always good, as was already pointed out in reference 3, and Kivel's widths are too large, although not by an order of magnitude.

In the case of lines emitted by ions, the situation is a little different, but the result<sup>6,7</sup> is again that, in practical cases, the classical path theory is valid. Actually, the calculation of  $\sigma_i$  by quantum mechanical perturbation theory is often valid too, provided one replaces the plane waves of the Born approximation by Coulomb wave functions, but then it gives the same result as the classical path approximation. The reason is that Coulomb effects decrease the contribution of small impact parameters and effectively introduce a  $\rho_{min}$  which is always larger than  $\lambda$ .

In a similar manner, Kivel's shift is the standard quantum mechanical answer given by second-order time-independent perturbation theory, and should be correct provided that perturbation theory hold for all impact parameters that make an important contribution. This is just the condition under which the high-velocity limit, Eq. (3.12), was derived, hence Kivel's shift should be identical with the imaginary part of Eq. (3.12), and it is. The foregoing comparison of the present work with Kivel's constitutes one more demonstration of the equivalence of the classical and

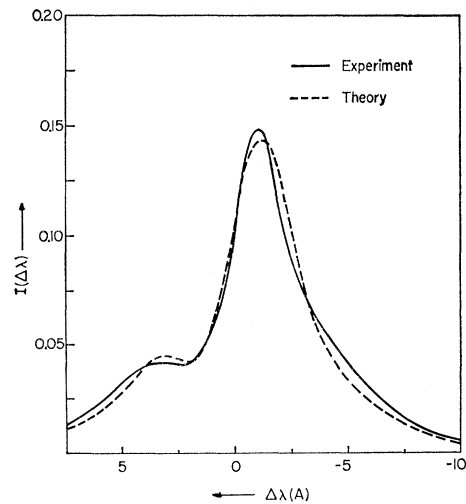


FIG. 4. Profile of the He I 3965 Å line at  $N = 2.5 \times 10^{16} \text{ cm}^{-3}$  and  $T = 30\,000^\circ\text{K}$ .

<sup>34</sup> R. Alpher and D. R. White, *Phys. Fluids* **2**, 162 (1959).  
<sup>35</sup> H. F. Berg, A. W. Ali, R. Lincke, and H. R. Griem, this issue [*Phys. Rev.* **125**, 199 (1962)].  
<sup>36</sup> M. Rudkjöbing, *Ann. Astrophys.* **12**, 229 (1949).  
<sup>37</sup> B. Kivel, *Phys. Rev.* **98**, 1055 (1955).

quantum mechanical theories in their common domain of validity.<sup>21</sup>

Some work very similar in spirit to the present one is due to Vainshtein and Sobel'man.<sup>38</sup> Unfortunately, their improper handling of the  $m$  degeneracy and their wrong choice of the interaction potential [see their Eq. (9)] invalidate all their numerical results. They also treat the ions by the impact theory, which is often a bad approximation for laboratory plasmas. One might mention an interesting way of performing the cutoff at small  $\rho$  [see their Eq. (15)], which is more elegant than the one used here but also involves more numerical work, without ensuring a significant improvement in accuracy. Finally, Vainshtein and Sobel'man suggest that one should use the shifts rather than the widths for the determination of electron densities. This suggestion is based on the notion that the calculation of widths, which are caused mainly by inelastic collisions, requires a quantum mechanical treatment of the electron motion, while it is not so important for the shifts, which are due mostly to elastic collisions. They question the validity of their semiclassical calculations and feel that nothing short of a full quantum mechanical analysis will be adequate [see in particular the discussion following their Eq. (19)]. However, it should be pointed out again that the theory they are developing is actually identical to the quantum mechanical one under appropriate conditions, and that both shifts and widths are correctly given by the semiclassical theory, even when there are collision-induced transitions. Furthermore, the numerical accuracy in computing the widths is greater than for the shifts (which can be very small), so that greater reliability in diagnostic determinations is expected from a calculation of the width or of the whole profile. (For a further discussion of this point, see reference 24.)

#### APPENDIX X

The equivalent cutoff is critical only when the exponentials in Eq. (2.15) are approximately unity, i.e., when the levels  $\alpha, \alpha', \dots$  are degenerate or near-degenerate. Otherwise, the exponentials themselves provide convergence for large  $\rho$ . They will therefore be ignored here. The average over angles of  $E_{1\sigma}(u_1)E_{1\nu}(u_2)$  is equal to  $\frac{1}{3}\mathbf{E}_1(u_1)\cdot\mathbf{E}_1(u_2)$ . In the second-order term of Eq. (2.15), the integral over  $u_2$  can be extended all the way to  $+\infty$  if one inserts a factor  $\frac{1}{2}$ . Therefore, the equivalent cutoff is defined by

$$\int_{\epsilon}^{+\infty} \rho d\rho \int_{-\infty}^{+\infty} du_1 \int_{-\infty}^{+\infty} du_2 \mathbf{E}_{1s}(u_1) \cdot \mathbf{E}_1(u_2) \\ = \int_{\epsilon}^{\rho_c} \rho d\rho \int_{-\infty}^{+\infty} du_1 \int_{-\infty}^{+\infty} du_2 \mathbf{E}_1(u_1) \cdot \mathbf{E}_1(u_2), \quad (\text{X1})$$

<sup>38</sup> L. A. Vainshtein and I. I. Sobel'man, Optics and Spectroscopy (USSR) VI, 440 (1959).

where the subscript  $s$  indicates a shielded field, all other fields being unshielded. The impact parameter  $\epsilon$  is supposed to be very small compared to the Debye length  $\rho_D$ . It cannot be taken zero, because the integral would diverge. Since the time of closest approach is zero, one has

$$\mathbf{E}_1(u_1) \cdot \mathbf{E}_1(u_2) \\ = e^2(\rho^2 + v^2 u_1 u_2)(\rho^2 + v^2 u_1^2)^{-\frac{3}{2}}(\rho^2 + v^2 u_2^2)^{-\frac{3}{2}}; \\ \mathbf{E}_{1s}(u_1) \cdot \mathbf{E}_1(u_2) \\ = \mathbf{E}_1(u_1) \cdot \mathbf{E}_1(u_2) [1 + (\rho^2 + v^2 u_1^2)^{\frac{1}{2}}/\rho_D] \\ \times \exp[-(\rho^2 + v^2 u_1^2)^{\frac{1}{2}}/\rho_D]. \quad (\text{X2})$$

After some elementary integrations, (X1) becomes

$$\int_{\epsilon}^{+\infty} \rho d\rho \int_{-\infty}^{+\infty} du_1 (\rho^2 + v^2 u_1^2)^{-\frac{3}{2}} [1 + (\rho^2 + v^2 u_1^2)^{\frac{1}{2}}/\rho_D] \\ \times \exp[-(\rho^2 + v^2 u_1^2)^{\frac{1}{2}}/\rho_D] = \frac{2}{v} \ln(\rho_c/\epsilon). \quad (\text{X3})$$

The integral over  $u_1$  can be done by parts and yields  $(2/v\rho\rho_D)K_1(\rho/\rho_D)$ . Then the integral over  $\rho$  can be performed and (X3) reduces to

$$K_0(\epsilon/\rho_D) = \ln(\rho_c/\epsilon). \quad (\text{X4})$$

Using the first term in the expansion of  $K_0$  for small argument

$$K_0(\epsilon/\rho_D) \simeq \ln(2\rho_D/\gamma\epsilon), \quad \gamma = 1.781, \quad (\text{X5})$$

yields for the value of the equivalent cutoff

$$\rho_c = 2\rho_D/\gamma = 1.123\rho_D.$$

#### APPENDIX Y

In this Appendix the integrals appearing in the calculation of width and shift are evaluated. According to Eq. (3.6) one has

$$f(z) \equiv A(z) + iB(z) \\ = \frac{1}{2} \left[ \int_{-\infty}^{+\infty} \frac{dx_1 e^{izx_1}}{(1+x_1^2)^{\frac{3}{2}}} \int_{-\infty}^{x_1} \frac{dx_2 e^{-izx_2}}{(1+x_2^2)^{\frac{3}{2}}} \right. \\ \left. + \int_{-\infty}^{+\infty} \frac{dx_1 x_1 e^{izx_1}}{(1+x_1^2)^{\frac{3}{2}}} \int_{-\infty}^{x_1} \frac{dx_2 x_2 e^{-izx_2}}{(1+x_2^2)^{\frac{3}{2}}} \right], \quad (\text{Y1})$$

where  $A(z)$  and  $B(z)$  are real functions.

On decomposing the exponentials the real part becomes

$$A(z) = \left( \int_0^{\infty} \frac{\cos zx}{(1+x^2)^{\frac{3}{2}}} dx \right)^2 + \left( \int_0^{\infty} \frac{x \sin zx}{(1+x^2)^{\frac{3}{2}}} dx \right)^2 \\ = \left( \int_0^{\infty} \frac{\cos zx}{(1+x^2)^{\frac{3}{2}}} dx \right)^2 + \left( \frac{d}{dz} \int_0^{\infty} \frac{\cos zx}{(1+x^2)^{\frac{3}{2}}} dx \right)^2. \quad (\text{Y2})$$



With the relations<sup>39</sup>

$$\int_0^\infty \frac{\cos zx}{(1+x^2)^{\frac{3}{2}}} dx = |z| K_1(|z|), \tag{Y3}$$

and

$$\frac{d}{dz} \int_0^\infty \frac{\cos zx}{(1+x^2)^{\frac{3}{2}}} dx = -\frac{d}{dz} (|z| K_1(|z|)) = -z K_0(|z|), \tag{Y4}$$

one obtains finally Eq. (3.7).

To evaluate the imaginary part  $B(x)$ , one considers the function

$$L(z) = \int_{-\infty}^{+\infty} \frac{f(z') dz'}{z' - z}, \tag{Y5}$$

where the path of integration is the real axis, except for a small detour above the singularity of  $f(z')$  at  $z'=0$ . Now  $f(z)$  is obviously analytic in the upper half plane because  $|e^{izx_1}|$  is always smaller than  $|e^{izx_2}|$ ,  $x_1$  being the upper limit of the integration over  $x_2$ . Therefore the path of integration can be closed above and, for  $z$  in the upper half plane, Cauchy's theorem gives

$$L(z) = 2\pi i f(z). \tag{Y6a}$$

But, for  $z$  tending to the real axis, one can also write  $L(z)$  as the sum of a principal-value integral and of the contribution from a small semicircle around the pole

$$L(z) = P \int_{-\infty}^{+\infty} \frac{f(z') dz'}{z' - z} + \pi i f(z). \tag{Y6b}$$

From the comparison of these two expressions it follows for real  $z$  that

$$f(z) = \frac{1}{\pi i} P \int_{-\infty}^{+\infty} \frac{f(z') dz'}{z' - z}. \tag{Y7}$$

Now  $A(z)$ , i.e., the real part of  $f(z)$ , is obviously even, and taking the imaginary part of (Y7) yields

$$\begin{aligned} B(z) &= -P \int_{-\infty}^{+\infty} \frac{A(z')}{z - z'} dz' \\ &= -P \int_{-\infty}^{+\infty} \frac{A(z')}{z + z'} dz' \\ &= -P \int_{-\infty}^{+\infty} \frac{A(z')}{z^2 - z'^2} dz' \\ &= -P \int_0^\infty \frac{A(z')}{z^2 - z'^2} dz', \end{aligned} \tag{Y8}$$

which is Eq. (3.8).

<sup>39</sup> G. N. Watson, *Theory of Bessel Functions* (Cambridge University Press, New York, 1952), 2nd ed., p. 172.

By two partial integrations, (3.8) can be brought into a form more suitable for numerical integration:

$$\begin{aligned} B(z) &= \frac{1}{\pi} \int_0^\infty [(z+z') \ln|z+z'| + (z-z') \ln|z-z'|] \\ &\quad \times [2K_0^2(z') - 8z'K_0(z')K_1(z') + 4z'^2(K_0^2(z') \\ &\quad + K_1^2(z'))] dz'. \end{aligned} \tag{Y9}$$

This formula was used to compute  $B(z)$  for  $z \geq 0.2$ . For smaller arguments the following version of (3.8) proved to be more convenient

$$B(z) = \frac{1}{\pi} \int_{-\infty}^{+\infty} \left[ \frac{A(z')}{z - z'} - \frac{A(z) A(z - z')}{A(0) z - z'} \right] dz'. \tag{Y10}$$

The second term has the same singularity as the first term, but integrates out to zero, because  $A(z)$  is an even function.

In order to extrapolate the numerical integrations for  $B(z)$  to zero, it was necessary to obtain the derivative  $[B'(z)]_{z=0}$  from (Y1).

$$\begin{aligned} B'(0) &= \frac{1}{2} \left[ \int_{-\infty}^{+\infty} \frac{dx_1 x_1}{(1+x_1^2)^{\frac{3}{2}}} \int_{-\infty}^{x_1} \frac{dx_2}{(1+x_2^2)^{\frac{3}{2}}} \right. \\ &\quad - \int_{-\infty}^{+\infty} \frac{dx_1}{(1+x_1^2)^{\frac{3}{2}}} \int_{-\infty}^{x_1} \frac{dx_2 x_2}{(1+x_2^2)^{\frac{3}{2}}} \\ &\quad + \int_{-\infty}^{+\infty} \frac{dx_1 x_1^2}{(1+x_1^2)^{\frac{3}{2}}} \int_{-\infty}^{x_1} \frac{dx_2 x_2}{(1+x_2^2)^{\frac{3}{2}}} \\ &\quad \left. - \int_{-\infty}^{+\infty} \frac{dx_1 x_1}{(1+x_1^2)^{\frac{3}{2}}} \int_{-\infty}^{x_1} \frac{dx_2 x_2^2}{(1+x_2^2)^{\frac{3}{2}}} \right] \\ &= \frac{1}{2} \left[ \int_{-\infty}^{+\infty} \frac{x^2 dx}{(1+x^2)^2} \int_{-\infty}^{+\infty} \frac{dx}{(1+x^2)^2} \right. \\ &\quad \left. - \int_{-\infty}^{+\infty} \frac{x \ln[x + (1+x^2)^{\frac{1}{2}}] dx}{(1+x^2)^{\frac{3}{2}}} \right] = 0. \end{aligned} \tag{Y11}$$

One might suspect this result because it involves an infinite integral, namely

$$\int_{-\infty}^{x_1} \frac{x_2^2 dx_2}{(1+x_2^2)^{\frac{3}{2}}} = \left[ \ln[x_2 + (1+x_2^2)^{\frac{1}{2}}] - \frac{x_2}{(1+x_2^2)^{\frac{1}{2}}} \right]_{-\infty}^{x_1}.$$

However, the contribution to  $B'(0)$  from the lower

limit of this integral,

$$\begin{aligned} \lim_{x, x' \rightarrow \infty} \frac{1}{2} \int_{-x}^{+x'} \frac{dx_1 x_1}{(1+x_1^2)^{3/2}} & \left( \ln[-x + (1+x^2)^{1/2}] + \frac{x}{(1+x^2)^{1/2}} \right) \\ &= \frac{1}{2} \lim_{x, x' \rightarrow \infty} \left[ \frac{-1}{(1+x_1^2)^{3/2}} \right]_{-x}^{+x'} \left( \ln \frac{1}{2x^2} + 1 \right) \\ &= \frac{1}{2} \lim_{x, x' \rightarrow \infty} \left( \frac{1}{x} - \frac{1}{x'} \right) \left( \ln \frac{1}{2x^2} + 1 \right), \end{aligned}$$

vanishes and (Y11) is indeed correct.

The functions  $a(z)$  and  $b(z)$  defined by Eq. (3.9) were calculated numerically from  $A(z)$  and  $B(z)$ . It is possible to obtain  $b(0)$  in closed form by writing

$$\begin{aligned} b(\epsilon) &= \int_{\epsilon}^{\infty} \frac{B(z)}{z} dz = -\frac{1}{\pi} \int_{\epsilon}^{\infty} \frac{dz}{z} \int_{-\infty}^{+\infty} \frac{A(z')}{z-z'} dz' \\ &= -\frac{1}{\pi} \lim_{\eta \rightarrow 0} \int_{\epsilon}^{\infty} \frac{dz}{z} \operatorname{Re} \int_{-\infty}^{+\infty} \frac{A(z')}{z-z'-i\eta} dz'. \end{aligned} \quad (\text{Y12})$$

Interchanging the order of integration gives

$$\begin{aligned} b(\epsilon) &= -\frac{1}{\pi} \lim_{\eta \rightarrow 0} \int_{-\infty}^{+\infty} dz' A(z') \operatorname{Re} \int_{\epsilon}^{\infty} \frac{dz}{z(z-z'-i\eta)} \\ &= -\frac{1}{\pi} \lim_{\eta \rightarrow 0} \int_{-\infty}^{+\infty} dz' A(z') \operatorname{Re} \left( \frac{1}{z'+i\eta} \right) \\ & \quad \times \left[ \ln(z-z'-i\eta) - \ln z \right]_{\epsilon}^{\infty} \\ &= -\frac{1}{\pi} \lim_{\eta \rightarrow 0} \int_{-\infty}^{+\infty} dz' A(z') \left( \frac{\eta}{z'^2 + \eta^2} \right) \tan^{-1} \left( \frac{\eta}{\epsilon - z'} \right). \end{aligned} \quad (\text{Y13})$$

(All the other terms give no contribution to the integral over  $z'$ .) Taking the limit  $\epsilon \rightarrow 0$  leads to

$$b(0) = -\frac{1}{\pi} \lim_{\eta \rightarrow 0} \int_{-\infty}^{+\infty} dz' A(z') \frac{\eta}{z'^2 + \eta^2} \tan^{-1} \left( \frac{\eta}{-z'} \right). \quad (\text{Y14})$$

For small  $\eta$ , all the contribution arises from  $z'$  near zero so that  $A(z')$  can be replaced by  $A(0)=1$ . The remaining integral is elementary and gives finally

$$b(0) = \pi/2. \quad (\text{Y15})$$

It can also be shown that  $a(z)$  diverges logarithmically for small  $z$ , i.e.,

$$a(z) = \int_z^{\infty} \frac{A(z')}{z'} dz' \rightarrow \ln(1/|z|). \quad (\text{Y16})$$

For large  $z$  the asymptotic behavior of  $A(z)$  and  $B(z)$  (the adiabatic limit) follows from (3.7) and (Y1), respectively, as

$$A(z) \sim \pi |z| e^{-2|z|}; \quad B(z) \sim \pi/4z. \quad (\text{Y17})$$

The corresponding relations for  $a(z)$  and  $b(z)$  are

$$a(z) \sim (\pi/2) e^{-2|z|}; \quad b(z) \sim \pi/4z. \quad (\text{Y18})$$

## APPENDIX Z

With the Holtmark result<sup>40</sup> for the field strength distribution function

$$W(\beta) = \frac{2}{\pi} \int_0^{\infty} \sin(\beta\eta) \exp(-\eta^3) \eta d\eta, \quad (\text{Z1})$$

the reduced profile of an isolated line in the quasi-static approximation for ions follows from Eq. (4.14) after inverting the order of integrations as

$$\begin{aligned} j_H(x, \alpha) &= \frac{2}{\pi^2} \int_0^{\infty} d\eta \eta \exp(-\eta^3) \\ & \quad \times \int_0^{\infty} d\beta \frac{\beta \sin(\beta\eta)}{1 + [x - (\alpha)^{2/3} \beta^2]^2}. \end{aligned} \quad (\text{Z2})$$

This can also be written

$$\begin{aligned} j_H(x, \alpha) &= \frac{|\alpha|^{-8/3}}{\pi^2} \int_0^{\infty} d\eta \eta \exp(-\eta^3) \operatorname{Im} \int_{-\infty}^{\infty} d\beta \\ & \quad \times \frac{\beta e^{i\beta\eta}}{(A_+ + i\beta)(A_+ - i\beta)(A_- + i\beta)(A_- - i\beta)}, \end{aligned} \quad (\text{Z3})$$

where  $A_+$  and  $A_-$  are defined by

$$A_{+,-} \equiv |\alpha|^{-3} (\delta |x| > \pm i)^{1/2}, \quad (\text{Z4})$$

with  $\delta = -1$  for  $x/\alpha > 0$ ,  $\delta = +1$  for  $x/\alpha < 0$ . Then one has

$$A_{+,-} = |\alpha|^{-3} (R_{\pm} \pm iR_{\pm}), \quad (\text{Z5})$$

with  $R_+$  and  $R_-$  given by

$$R_{+,-} = [\pm \delta |x| + (1+x^2)^{1/2}]^{1/2} \sqrt{2}. \quad (\text{Z6})$$

In terms of these quantities the profile is

$$\begin{aligned} j_H(x, \alpha) &= -\frac{1}{2\pi^2} \int_0^{\infty} d\eta \eta \exp(-\eta^3) \frac{\alpha^{-2}}{R_-} \\ & \quad \times \operatorname{Im} \int_{-\infty}^{\infty} d\beta \frac{\beta e^{i\beta\eta}}{(\beta + iA_+)(\beta + iA_-)} \\ & \quad \times \left( \frac{1}{\beta - iA_+} - \frac{1}{\beta - iA_-} \right). \end{aligned} \quad (\text{Z7})$$

A contour integration encircling the simple poles at  $iA_+$  and  $iA_-$  yields

$$\begin{aligned} j_H(x, \alpha) &= \frac{|\alpha|^{-3}}{\pi} \int_0^{\infty} d\eta \eta \exp[-\eta^3 - R_+ \eta |\alpha|^{-3}] \\ & \quad \times \sin(R_- \eta |\alpha|^{-3}). \end{aligned} \quad (\text{Z8})$$

<sup>40</sup> J. Holtmark, Ann. Physik **58**, 577 (1919).

Asymptotic formulae for the line wing can be obtained by expanding  $\exp(-\eta^2)$  and integrating term by term:

$$j_H(x,\alpha) = -\frac{1}{\pi} \sum_{n=1}^{\infty} (-1)^{n-1} \times \frac{\Gamma(\frac{1}{2}(3n+1)) |\alpha|^{n-1} \sin[\frac{1}{2}(3n+1)(\tan^{-1}(R_-/R_+))]}{\Gamma(n)(1+x^2)^{(3n+1)/8}}. \tag{Z9}$$

The first two terms are

$$j_H(x,\alpha) = \frac{1}{\pi(1+x^2)} - \frac{15}{8\sqrt{\pi}} \frac{\alpha}{(1+x^2)^{7/8}} \times \sin\left[\frac{7}{2} \tan^{-1}(-\delta|x| + (1+x^2)^{1/2})\right]. \tag{Z10}$$

For large  $x$  one has finally

$$j_H(x,\alpha) \simeq \frac{1}{\pi x^2} + \frac{15\alpha}{8(2\pi)^{1/2} x^{7/4}} + \dots \simeq \frac{1}{\pi x^2} + \frac{3\alpha}{4x^{7/4}} + \dots, \tag{Z11}$$

if  $x/\alpha > 0$  and

$$j(x,\alpha) \simeq 1/\pi x^2, \tag{Z12}$$

if  $x/\alpha < 0$ . Here the ion effects are not important.

That Eqs. (Z11) and (Z12) agree with the first two terms of the wing expansion of Eq. (4.11), which involved the scalar additivity assumption, can be seen by expanding  $\exp[-i^{1/2}\Gamma(\frac{1}{4})\alpha\tau^{3/2}]$  in this equation and integrating term by term. Up to this order also the time-dependent theory yields the same result, which can be shown by expanding the phase integral in a power series of the time if one notices that the first-order term gives the quasi-static approximation, Eq. (4.11).